COMMUN. MATH. SCI.
Vol. 8, No. 2, pp. 481–517


# TWO COARSE-GRAINING STUDIES OF STOCHASTIC MODELS IN MOLECULAR BIOLOGY*

PETER R. KRAMER†, JUAN C. LATORRE‡, AND ADNAN A. KHAN§

*Dedicated to Andy Majda with gratitude and admiration*

**Abstract.** We examine stochastic coarse-graining strategies for two biomolecular systems. First, we compute the large-scale transport properties of the basic flashing ratchet mathematical model for (Brownian) molecular motors and consider in this light whether the underlying continuous-space, continuous-time Markovian model can be coarse-grained as a discrete-state, continuous-time Markovian random walk model. Through careful computation of associated statistical signatures of Markovianity, we find that such a discrete coarse-graining is an excellent approximation over much but not all of the parameter regime. In particular, for the parameter values associated with the fastest transport by the flashing ratchet, the discretized model displays non-Markovian features such as waiting times between jumps which are not exponentially distributed. We provide a theoretical framework for understanding the conditions under which Markovianity is to be expected in the discretized model and two mechanisms by which the flashing ratchet model coarse-grains to a non-Markovian discretized model. Next we turn to a basic question of how the dynamics of water molecules near the surface of a solute can be represented by a simple drift-diffusion stochastic model. This question is of most interest for the purpose of accelerating molecular dynamics simulations of proteins, but for simplicity, here we examine the simple case where the solute is a $C_{60}$ buckyball, which has a homogenous, roughly isotropic form. We compare the mathematical drift-diffusion framework with a statistical quantification of water dynamics near a solute discussed in the biophysical literature. A key concern is the choice of time interval on which to sample the molecular dynamics data to generate estimators for the drift and diffusivity. We use a simple mathematical toy model to establish insight and a strategy, but find for the actual molecular dynamics data that the sampling times which produce the most faithful drift coefficient and the sampling times which produce the most faithful diffusion coefficient do not overlap, so that sacrifice of quality in one or the other parameter appears necessary.

**Key words.** Brownian motors, molecular dynamics, stochastic parameterization, continuous-time random walk, coarse-graining.

**AMS subject classifications.** 60G50, 60G51, 60J27, 60J60, 60J70, 60K15, 60K20, 60K37, 62M05, 62P10, 82C05, 82C31, 82C41, 92C17, 92C40, 92C45

## 1. Introduction

In this article, we present two stochastic models for processes in molecular biology which reflect the spirit of Andy's influence on my (PRK's) research. Both are mathematically abstracted and simplified frameworks for which fundamental questions can be examined in a more transparent manner than more detailed and realistic models. The first modeling framework to be examined is the flashing ratchet model (section 2) for molecular motors — proteins in the biological cell such as kinesin, myosin, and dynein which convert chemical and thermal energy into useful mechanical work for

*Received: December 21, 2008; accepted (in revised version): June 3, 2009.
This work was supported by NSF CAREER grant DMS-0449717. PRK and JCL would also like to acknowledge the hospitality and support of the Institute for Mathematics and Its Applications at the University of Minnesota, at which part of this work was developed.

†Department of Mathematical Sciences, Rensselaer Polytechnic Institute, 110 8th St., Troy, NY 12180, USA (kramep@rpi.edu).

‡Institute of Mathematics, Freie Universität Berlin, Arnimallee 6, 14195 Berlin, Germany (latorre@mi.fu-berlin.de).

§Department of Mathematics, Lahore University of Management Sciences, Lahore Cantt, 54792, Pakistan (adnan.khan@lums.edu.pk).

cell locomotion, polymerization, and muscular contraction. Of course each biological molecular motor has its own particular features which govern how it operates in detail, but unifying mechanisms have been theoretically identified and developed over the last decade or two [49, 50, 1, 19, 40, 26, 18]. Beyond providing simplified and abstract descriptions for the operation of molecular motors, these mathematical modeling frameworks have provided a great deal of stimulus for posing and addressing theoretical questions in stochastic modeling and nonequilibrium statistical mechanics [48, 35, 43, 49, 11, 10]. Our objective here falls within this purview as, after a description of the effective transport properties of the flashing ratchet (section 3), we examine the question of the extent to which flashing ratchet models for molecular motors can be accurately coarse-grained in terms of Markovian continuous-time random walks (MCTRW) on a discrete spatial lattice. Such an approximation is naturally motivated by the spatially periodic structure of the flashing ratchet model with dichotomous multiplicative noise (presented in section 2) and the Markovianity of the underlying detailed flashing ratchet model. Moreover, the use of Markovian continuous-time random walk models for molecular motors is prevalent in the literature [35, 13, 25], and naturally raises the question as to how such models are related to the more detailed stochastic differential equation models such as flashing ratchets (section 4). The work [23] rigorously studied a related approximation of a periodically (rather than randomly) flashing ratchet model by a *discrete-time* Markov chain with epochs marked by a sequence of times with regular deterministic spacing. In [32], the statistics of a discretized renewal process associated with visits to successive local minima of a static (non-flashing) periodic potential with applied force (or tilt) were explored. We find that in fact over a wide parameter regime, the MCTRW models do provide excellent approximations to the flashing ratchet model, but also identify regimes in which they do not. Most notably, the parameter regime for which motor transport is fastest is not well approximated by a MCTRW. A close consideration suggests that what is needed for a MCTRW model to be appropriate is that the motor makes many approximately independent attempts to pass the barrier into a neighboring well of the potential. We identify two different regimes where the MCTRW approximation is not valid, and identify different mechanisms for the violation of the needed condition. In one regime, the motor doesn't equilibrate within a potential well fast enough before it moves to a neighboring well. In the second regime, the motor does equilibrate within each well, but typically escapes after only a few flashing cycles, so only makes an $O(1)$ number of independent attempts to cross into the neighboring well. These conclusions are developed through a combination of some elementary probability considerations (section 5), numerical solution of deterministic equations for statistics of the motor transport (section 5.1), and direct Monte Carlo simulation of motor trajectories. In the course of the analysis, we identify a subtle point in the computation of the rates of jumping between wells in terms of exit times, which has sometimes been overlooked in the literature (Appendix A). Our findings are summarized in section 6.

We next turn to an initial effort at developing a stochastic dynamical model for the behavior of water molecules surrounding a solute (section 7). The quest to obtain simplified statistical description of water molecules is motivated by the desire to cut down on the substantial computational expense incurred by the need to account for the presence of solvent (i.,e., water) molecules for accurate molecular dynamics simulations of proteins [51, 36, 55, 2, 33]. The actual dynamics of the water molecules are of secondary interest, so one would like to represent the effects of the water molecules

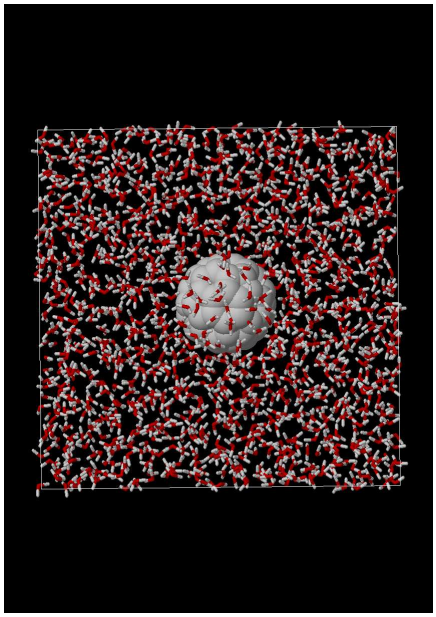

FIG. 1.1. *Snapshot of molecular dynamics simulation with 4200 "simple point charge" water molecules surrounding a $C_{60}$ buckyball.*

on the protein without resolving the water molecules explicitly. One reason for hope that this is possible is that the space and time scales characterizing the dynamics of water molecules ($10^{-10}$ m and $10^{-11}$ – $10^{-8}$ s) are often considerably smaller than those characterizing conformational changes in the protein molecule ($10^{-9}$ – $10^{-8}$ m and $10^{-10}$ – $10^{-3}$ s) [22, 36, 12, 17, 51, 38]. When combined with the observation that the water involves a greater number of degrees of freedom than the protein, one might try to view the water molecules in statistical mechanical terms as existing at every moment of time in some sort of local equilibrium determined by the momentary structure of the protein molecule. The relatively slow dynamics of the protein molecule will be influenced by this locally equilibrated environment, and as the protein's conformation changes, the statistics of the surrounding water will move rapidly (and possibly adiabatically) toward new equilibria. The notion of local equilibrium of the water molecules is of course dynamical and statistical. The statistical mechanical viewpoint, however, cannot be applied too literally with confidence. Indeed, while the space and time scales of the water molecules and protein molecule enjoy some degree of separation, and while many water molecules are present per degree of freedom of the protein, the aqueous environment cannot simply be thought of as some thermal heat bath. This point of view can capture some of the kinetic effects of the water molecules, but misses the important effects of hydrogen bonding and other chemical interactions between the water and protein molecules [4, 2, 16]. This suggests developing a model incorporating dynamical information beyond single-time statistics. A stochastic approach is strongly suggested because at the small scales of the protein molecule, the water molecules behave like discrete objects moving irregularly due to thermal and other effects and the protein molecule is itself undergoing thermal fluctuations.

As an initial step, we consider the development of a stochastic dynamical model for a water molecule near a buckyball, a solute much simpler than any protein, for the purpose of identifying and addressing some of the foundational issues. The buckyball (figure 1.1) is an approximately spherical configuration of carbon atoms, and therefore has the virtue of being both approximately isotropic and chemically homogenous. Consequently, the statistical behavior of water molecules near such a solute should depend only on its distance from the center (or surface) of the buckyball. Even in this vastly simplified setting, a number of interesting questions arise in the choice and parameterization of a statistical model. The first question is how to quantify the water dynamics as a function of distance from the solute. The biophysical literature [37, 34] seems to favor a description in terms of a spatially dependent diffusivity, which is physically natural, but the definition of the local diffusivity appears awkward (section 7). We adopt the more natural framework of diffusion processes from the theory of stochastic processes, in which the motion of a water molecule is decomposed into a spatially dependent drift and diffusivity. Within this framework, we develop the parameterization based on the definitions of the drift and diffusivity coefficients from the theory of stochastic processes (section 8). Caution is required though because the definitions refer to infinitesmal time intervals, and a naive implementation using the numerical time step instead is numerically inconsistent. Rather, the drift and diffusivity must be evaluated over time intervals which are short compared to the dynamics of the position variables, yet large enough that the drift-diffusion model is an even plausible approximation. The source of the latter restriction is similar to that in continuum field theory; the spatial and temporal derivatives refer to space and time differences which are small compared to the macroscale, yet large relative to the molecular scale. The appropriate time scale for computing drift and diffusivity of the water molecules is however not nearly as easy to identify as in classical fluid and solid mechanics — the range of valid choices is relatively restricted, and its upper and lower limits are not so clear *a priori*. Similar issues have been investigated mathematically in related multiscale frameworks [47, 46, 42].

For our purposes, we use an elementary, exactly solvable stochastic differential system as a tool for clarifying the choice of time scale in the computation of effective drift and diffusivity (section 9). We are particularly interested in being able to determine this sampling time scale without *a priori* knowledge about the precise values of the putative fast and slow time scales in the system. We observe from the toy model that the best choice of time scale appears to be that for which the computed coefficient has the largest magnitude (relative to other choices of time scales). This criterion is simple enough to be employed in a complex system (such as a molecular dynamics simulation) for which the fast and slow time scales may not be so easily determined *a priori* (due to complications from interacting with the solute boundary, for example). Applying this idea to data obtained from molecular dynamics simulations of water molecules near a buckyball, we find that the window of good time scales for the drift does not overlap with that for the diffusivity. As using a different time scale for each coefficient raises concerns of consistency, we choose a time scale for which the diffusivity appears well modeled, and sacrifice precision in the drift coefficient. This choice turns out to be quite a bit smaller than typical time values used in molecular dynamics to compute diffusivities (section 10).

## 2. Flashing ratchet model

An instructive mathematical abstraction for a class of molecular motors is the

flashing ratchet model [49, 41]:

$$\begin{aligned} \mathrm{d}X &= V\mathrm{d}t, \\ m\mathrm{d}V &= [-\gamma V - \phi'(X(t))F(t)]\,\mathrm{d}t + \sqrt{2\gamma k_B T}\mathrm{d}W(t). \end{aligned}$$

Here $X(t)$ denotes the position of the motor (here an idealized particle) along the track as a function of time $t$, and $V(t)$ denotes its velocity. Its dynamics are governed by a superposition of a flashing ratchet potential $\phi(x)F(t)$, a friction force (with coefficient $\gamma$), and thermal fluctuations characterized by Boltzmann's constant $k_B$, absolute temperature $T$, and the standard Wiener process $W(t)$, a Gaussian random process with the following formal stochastic calculus rules (Itô and Stratonovich interpretations are here equivalent) [15, Ch. 4]:

$$\begin{aligned} \langle \mathrm{d}W(t) \rangle &= 0, \\ \langle \mathrm{d}W(t)\mathrm{d}W(s) \rangle &= \delta(t-s)\mathrm{d}t\mathrm{d}s. \end{aligned}$$

Angle brackets $\langle\cdot\rangle$ denote statistical averages. The flashing ratchet potential $\phi(x)F(t)$ itself is spatially periodic ($\phi(x+L)=\phi(x)$) and modulated in amplitude by a continuous-time Markov chain $F(t)$. We will content ourselves with the simplest version in which the Markov chain $F(t)$ takes values $f_1=1$, corresponding to an "on" (static potential) state of the potential, and $f_2=0$, corresponding to an "off" (free diffusion) state of the potential. The flashing ratchet thereby acts as dichotomous multiplicative noise. The potential switches from off to on with transition rate $k_{21}$ and from on to off with transition rate $k_{12}$; equivalently, the mean lifetime of the off state is $k_{21}^{-1}$ and the mean lifetime of the on state is $k_{12}^{-1}$. The spatial periodicity of the potential reflects the typically periodic physical structure of the track along which the motor moves, while the modulation corresponds to chemically activated changes (such as ATP hydrolysis) in the interaction between motor and track. As the chemical processes rely on rare events involving interactions of a small number of molecules, they are naturally modeled as stochastic.

Because the molecular motor operates at such a small scale where frictional effects dominate inertia $m\phi'/(\gamma^2 L) \ll 1$, the following overdamped limit (obtained by a standard Smoluchowski reduction) [15, Sec. 6.4] is generally adequate:

$$\mathrm{d}X(t) = -\gamma^{-1}\phi'(X(t))F(t)\mathrm{d}t + \sqrt{\frac{2k_BT}{\gamma}}\,\mathrm{d}W(t). \tag{2.1}$$

Observe that because the state of the potential $F(t)$ has nontrivial temporal correlations, the motor particle trajectory $X(t)$ is not itself Markovian. Rather, the joint process $(X(t),F(t))$ is Markovian in the sense that conditioning upon the knowledge of the present state of these variables, the future and past evolution of these variables become independent [21, Sec. 1.3].

We non-dimensionalize the flashing ratchet model with respect to the spatial period length $L$ and the time scale $L^2\gamma/\bar{\phi}$, where $\bar{\phi}$ is the range of values of the potential, to obtain

$$\mathrm{d}X(t) = -\phi'(X(t))F(t)\mathrm{d}t + \sqrt{2\theta}\,\mathrm{d}W(t), \tag{2.2a}$$

where $\theta = k_BT/\bar{\phi}$ and we are using the same symbols for the non-dimensionalized functions as we previously did for their dimensional versions. Note that small values of $\theta$ correspond to systems in which the energy of thermal fluctuations is small compared

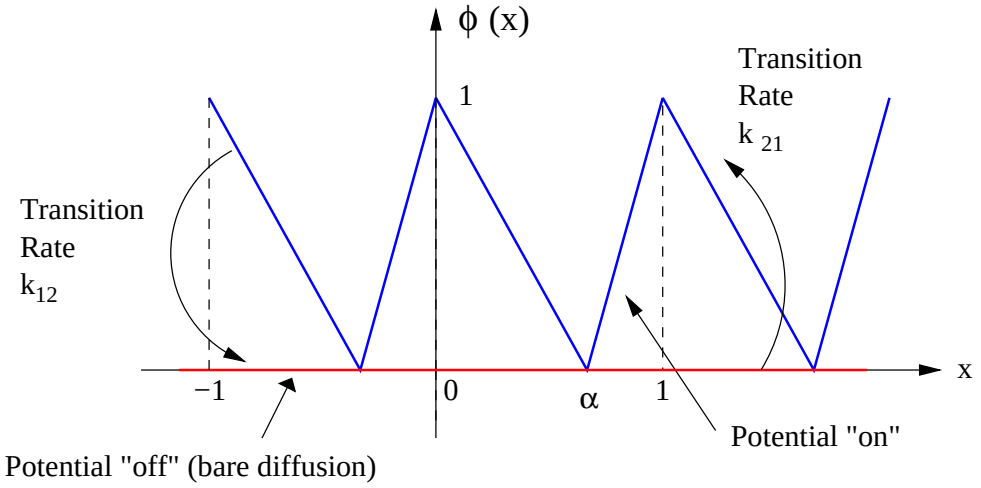


FIG. 2.1. *Piecewise linear potential for the flashing ratchet.*

to the height of the potential barrier; such moderately small values of $\theta$ are of primary interest in the study of molecular and Brownian motors.

For the subsequent analysis, we will take the simple asymmetric sawtooth potential shape

$$\phi(x) = \begin{cases} -\dfrac{x-\alpha}{\alpha} & \text{for} \quad 0 \le x < \alpha, \\ \dfrac{x-\alpha}{1-\alpha} & \text{for} \quad \alpha \le x < 1, \end{cases} \tag{2.2b}$$

repeated periodically with asymmetry parameter $\alpha$ describing the position of the potential minima (figure 2.1). One motivation for this choice is that we have control over the degree of asymmetry of the potential, as given by the parameter $\alpha$ (figure 2.1) specifying the minimum of the potential. We note that the equations for the statistics (Appendix A) for this potential can be expressed as a coupled system of ordinary differential equations with constant coefficients, which can formally be solved exactly up to a set of constants which need to be determined by the boundary conditions. However, as also noted by [27], the practical computation and use of this formally exact solution is actually more problematic than direct numerical solution of the equations.

For sufficiently weak noise $\theta$, the particle spends most of its time near a minimum $x \equiv \alpha \pmod{\mathbb{Z}}$ of the spatially periodic potential $\phi$, with occasional wanderings into a neighboring well (figure 2.2). The intuition [49] behind how the flashing ratchet model creates directed (useful) motion is that during an "on" period, the particle settles to the minimum of the valley in which it finds itself and is essentially trapped there until the potential turns off. Then the particle moves randomly via Brownian motion, and if it manages to wind up in the domain corresponding to a different valley of the potential, it will fall there when the potential turns back on. The asymmetry in the potential makes it easier for the particle to wander past the closer barrier during the off period, and therefore more likely to move in that direction (to the right for $\frac{1}{2} < \alpha < 1$). In this way, mean zero thermal fluctuations of the particle

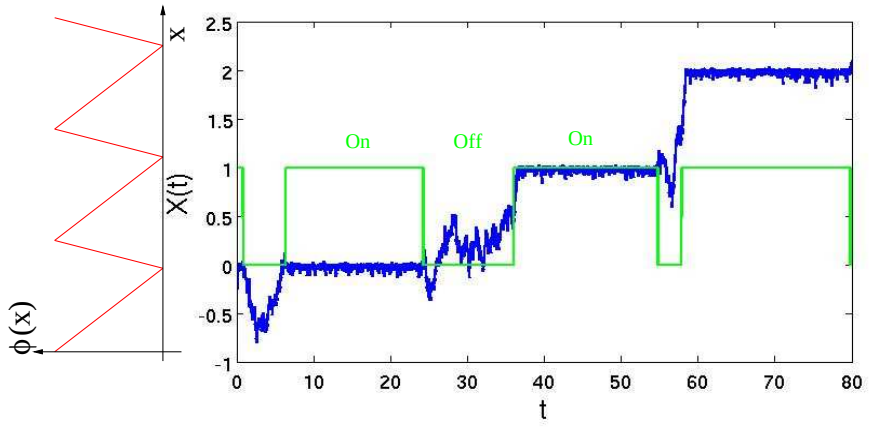


FIG. 2.2. *Sample trajectory of a flashing ratchet with dichotomous noise, equation (2.2).*

(with nondimensionalized amplitude parameterized by $\theta$) are rectified by the random fluctuations in the flashing potential to produce directed transport. Both the thermal fluctuations and the fluctuations in the potential are necessary; in the absence of either, the particle would have no mean motion. This extraction of useful work from noise is consistent with the second law of thermodynamics because an external energy input is required to flash the potential on and off and thereby do work on the motor particle.

## 3. Macroscopic transport parameters

The transport of the particle on the macroscale is naturally characterized by the effective drift

$$U = \lim_{t\to\infty} \frac{\langle X(t)\rangle}{t},$$

and effective diffusivity

$$D = \lim_{t\to\infty} \frac{\langle (X(t) - \langle X(t)\rangle)^2\rangle}{2t}.$$

As the particle's motion has short-range correlations, a central limit theorem argument implies that the probability distribution for its position at long times is approximately Gaussian, so the effective drift and diffusivity provide a sufficient description for the large-scale, long-time behavior [9].

The ratio

$$\mathrm{Pe} = \frac{|U|}{2D},$$

known as a Peclét number, provides a useful measure of the coherence of the transport. (Usually a factor of length appears in the numerator, but we have nondimensionalized the period length to 1). A small Peclét number implies noisy and incoherent transport,

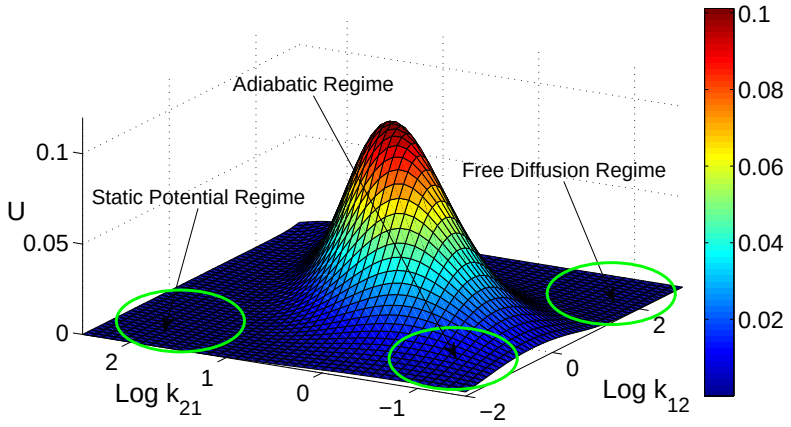


FIG. 3.1. *Effective drift as a function of* $k_{12}$ *and* $k_{21}$. $\theta = 10^{-1.5}$, $\alpha = 0.85$.

while a large Peclét number implies that the particle is moving nearly deterministically in a given direction. The Peclét number is related to a randomness parameter $r$ sometimes used to characterize the progress of a molecular motor [25, 13, 57] as $\mathrm{Pe} = 1/r$.

In figures 3.1 and 3.2 we plot landscapes for $U$ and Pe as functions of $k_{12}$ and $k_{21}$. In the landscape for $U$, we have labeled the common asymptotic regions found in the literature, such as the *static potential limit* ($k_{12} \to 0$) and the *adiabatic limit* ($k_{12}$, $k_{21} \to 0$) [49]. The more nontrivial dynamics occur away from these regions. In particular, both the drift $U$ and Peclét number Pe are maximized at intermediate values of the transition rates.

In figure 3.3, we show how the values $k_{12}^*$ and $k_{21}^*$ that maximize the Peclét number depend on the temperature $\theta$ for three different values of the potential minimum $\alpha$. For small temperatures $\theta \lesssim 10^{-1.5}$, we find a clean scaling for these optimal transition rates:

$$k_{12}^* \sim \mathrm{ord}(1), \quad k_{21}^* \sim \mathrm{ord}(\theta).$$

These scalings may be understood theoretically through the intuitive mechanism by which flashing ratchets operate [1, 49, 23]. Suppose we start observing the particle at the moment at which it is located near a potential minimum $x \equiv \alpha \pmod{\mathbb{Z}}$, where without loss of generality we will assume $1/2 < \alpha < 1$. When the potential turns off, the particle would have a decent chance of moving through pure diffusion to the region corresponding to the valley on the right (past the next integer value) if the potential remained off for at least a time scaling inversely with the temperature $\theta$. Extending the off-time of the potential substantially past this value just wastes time so we are led to suppose that the optimal rate for switching from the off to on state should behave like

$$k_{21}^* \sim \mathrm{ord}(\theta).$$

This is the scaling we observe in figure 3.3 for small temperatures. Once the particle crosses the potential maximum at $x \equiv 1 \pmod{\mathbb{Z}}$, the potential should turn on and

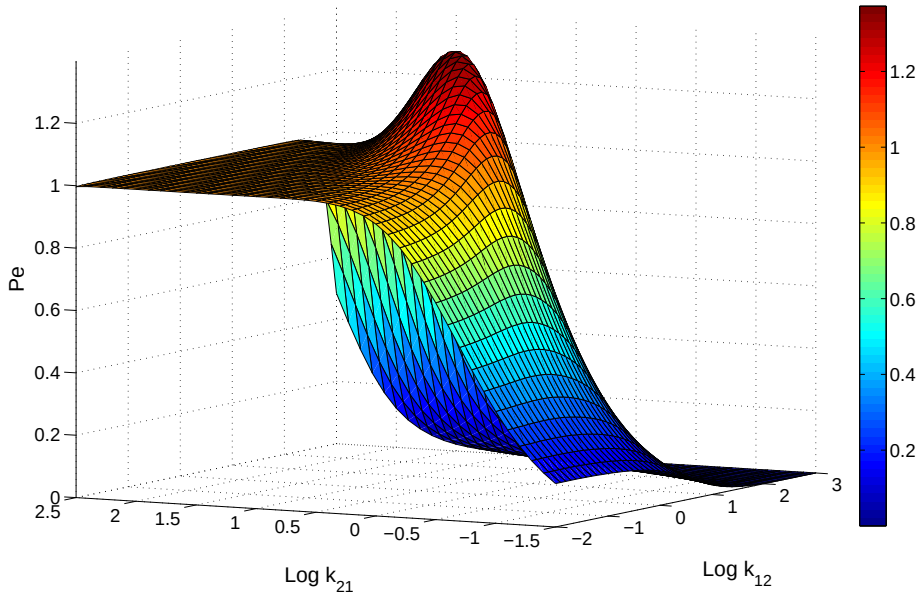


FIG. 3.2. *Peclét number as a function of* $k_{12}$ *and* $k_{21}$. $\theta = 10^{-1.5}$, $\alpha = 0.85$.

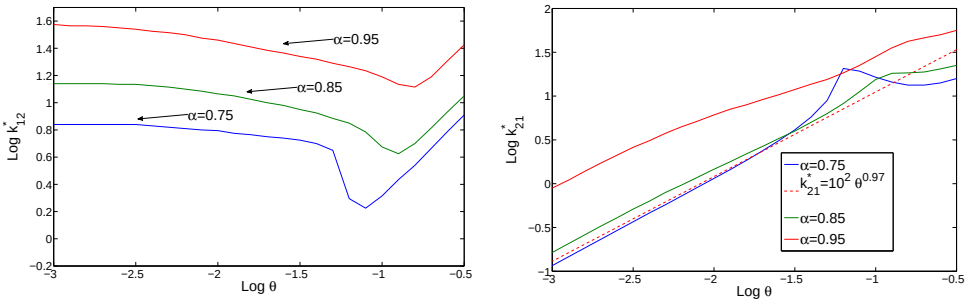


FIG. 3.3. *Value of* $k_{12}^*$ *(left) and* $k_{21}^*$ *(right) at which* Pe *is maximized.*

remain on for enough time so that the particle can be driven to reach the next minimum at $x \equiv (\alpha + 1) \pmod{\mathbb{Z}}$. For small temperature, this time is determined by the deterministic dynamics and is thus independent of temperature. Again, keeping the potential on for much longer than this time just inhibits the particle's motion, so we are led to suppose that

$$k_{12}^* \sim \mathrm{ord}(1),$$

which is the scaling we observe in figure 3.3 for $k_{12}^*$.

For reasons we do not understand satisfactorily, the behavior of the transition rates which optimize the drift (rather than the Peclét number) is qualitatively similar but with different scaling behavior than the above theoretical argument would

indicate. Details will be presented elsewhere; we note here simply that in general the regions of large drift substantially correspond with the regions of high Peclét number, but their peaks do not coincide nor scale in the same way with respect to the governing parameters.

The plots presented above were computed with 1000 grid points for each parameter using the procedure developed by [59, 58], which involves the solution of deterministic systems of equations related to the infinitesmal generator of the Markov process (2.1) governing the flashing ratchet. An alternative and equivalent framework based on homogenization theory was developed in [45, 28].

**4. Continuous-time random walk approximation**

The spatially periodic structure of the flashing ratchet model along with the particle trajectory's character of hovering near potential minima for most of the time suggests an intermediate coarse-graining of the flashing ratchet model in terms of a Markovian continuous–time random walk (MCTRW). The state space for the particle is condensed to the discrete lattice of potential minima, and its motion characterized through a sequence of integer indices of successive valleys visited $\{X_n\}_{n=0}^{\infty}$ and the times at which new potential valleys are visited $\{T_n\}_{n=0}^{\infty}$ (figure 4.1):

$$\begin{aligned} T_0 &= 0, \\ X_0 &= 0, \\ T_n &= \inf\{t > T_{n-1} : X(t) \in \alpha + \mathbb{Z}, X(t) \neq X_{n-1} + \alpha\}, \\ X_n &= X(T_n) - \alpha, \\ N(t) &= X_n \text{ for } T_n \leq t < T_{n+1}, n = 0, 1, 2, \ldots. \end{aligned} \tag{4.1}$$

Note that repeated visits to the same potential minimum are ignored if they are not separated by visits to other valleys.

The discretization (4.1) can always be done, but the interesting issue is its statistical properties. One might intuitively expect that the resulting approximate trajectory $N(t)$ would have the statistics of a Markovian continuous-time random walk, meaning that:

- the holding times $\Theta_n = T_n - T_{n-1}$ are independent, identically distributed random variables with exponential PDF $p_\Theta(t) = \langle\Theta\rangle^{-1} \mathrm{e}^{-t/\langle\Theta\rangle}$,
- the jumps $\Xi_n = X_n - X_{n-1}$ are independent, identically distributed random variables with probability distribution $\mathrm{Prob}(\Xi_n = 1) = \pi_+$, $\mathrm{Prob}(\Xi_n = -1) = 1 - \pi_+$,
- $\{\Theta_n\}_{n=0}^{\infty}$ and $\{\Xi_n\}_{n=0}^{\infty}$ are independent.

Markovianity of this coarse-grained process $N(t)$ is not guaranteed because the state $F(t)$ of the flashing ratchet is not included in the coarse-grained description. Yet one may still expect on intuitive grounds that the sequence of well visits $\{X_n\}_{n=0}^{\infty}$ to remain approximately Markovian. For example, by the strong Markov property, the sequence $\{X_n, F(T_n)\}_{n=0}^{\infty}$ is Markovian, and since the potential may generally be expected to be on during a new valley visit, the compression of information about the state of the potential may not be so crucial. This still raises the question of whether the holding times $\{\Theta_n\}_{n=0}^{\infty}$ should be exponentially distributed as one would generally expect for a steady potential with weak noise $\theta \ll 1$. Indeed, for simple diffusion (with no potential), the times beween visits to a new lattice site is not exponentially distributed [3]. We will find though that over a wide parameter regime, the MCTRW appears to be a good approximation in describing the particle's progress.

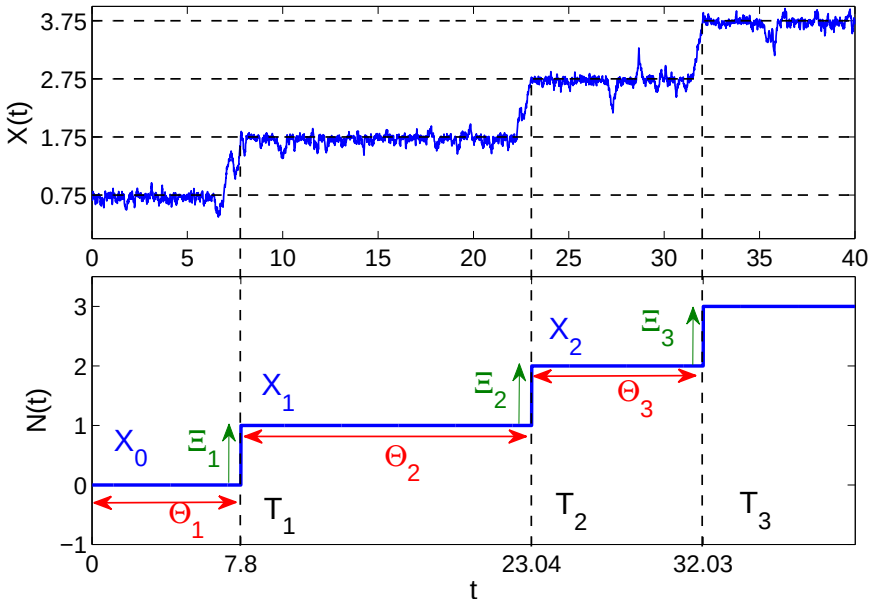


FIG. 4.1. *Discretization of trajectory of flashing ratchet.*

However, we also identify regimes where the MCTRW approximation loses validity for two different reasons, and the parameter range where motor transport is optimal falls within one of these regimes.

This can be immediately seen from the plot of the Peclét number with respect to transition rates in figure 3.2, realizing that for a MCTRW the drift and diffusion coefficients are given by the following expressions [15, Sec. 7.2]

$$U = \frac{\pi_+ - \pi_-}{\tau}, \qquad D = \frac{1}{2\tau},$$

so the Peclét number must satisfy

$$\mathrm{Pe} = |\pi_+ - \pi_-| \leq 1.$$

This inequality can also be shown to hold if the random walk were allowed to take steps of length greater than 1. We see the peak in the effective drift in figure 3.1 falls in a regime where $\mathrm{Pe} > 1$, which is inconsistent with a MCTRW model. On the other hand, we also see a wide regime where the Peclét number has a plateau $\mathrm{Pe} \approx 1$, which would be consistent with a MCTRW model with strong bias ($\pi_+ \gg \pi_-$ or vice versa). We next examine these regimes in microscopic detail using a combination of accurate numerical computations and some elementary probabilistic reasoning with an eye to understanding the mechanisms behind this observed behavior of the Peclét number.

## 5. Analysis of validity of MCTRW approximation

One way to understand whether the holding time of the particle between visits to new valleys is exponentially distributed is to conceptualize the transport from one valley to the next as the following sequence of events:

- The particle first relaxes to the minimum of the potential within its local valley. With the thermal noise, this could be said more precisely as the probability distribution of the particle relaxing to its stationary probability distribution within the local valley (with the barrier height imagined to be infinitely high so this stationary probability distribution exists).
- While the flashing ratchet is off, the particle diffuses freely, and may or may not escape past a neighboring peak location when the potential flashes back on.
- When the potential has flashed back on, the particle tends to be pushed back toward the potential minimum.
- After one or more cycles of the potential flashing back on, the particle essentially returns to the potential minimum (if it has not escaped to a neighboring valley yet) and starts anew.
- Eventually after several or many such escape attempts, the particle succeeds in passing a barrier location and then falling to a neighboring valley minimum as the potential flashes back on.

Clearly the particle must relax toward the minimum (or its local stationary distribution) on a short time scale compared with the time scale of its escape to the next valley if the jumping process from valley to valley is to have any Markovian character. Because the noise will generally be assumed small ($\theta \ll 1$), the relaxation time will be approximated in our considerations as $\tau^{(\mathrm{rel})} = 1/\alpha^2$ (for $1/2 < \alpha < 1$), the time for the particle to proceed by deterministically falling down the gradient from the peak to the valley (down the shallower slope).

If we assume this relaxation time is short compared to not only the holding time but also the typical time of a flashing cycle, we can use the above conceptual picture to represent the holding time as follows:

$$\Theta \sim \sum_{j=1}^{N_F} \Theta_j^{(\mathrm{f})} + \Theta^{(\mathrm{e})}, \tag{5.1}$$

where

- $N_F$ is (random) number of flash cycles before escape
- $\{\Theta_j^{(\mathrm{f})}\}$ are times between successive flash cycles of the potential,
- $\Theta^{(\mathrm{e})}$ is time taken to escape during the last flash period.

Suppose now that $N_F$ is large, meaning the particle is making many attempts to escape its valley during off cycles of the flashing potential before succeeding (figure 5.1). Assuming the particle is also resetting near the potential minimum many times, we may assume that $N_F$ is geometrically distributed (and approximately independent of the random times appearing in equation (5.1)). The times $\{\Theta_j^{(\mathrm{f})}\}$ between successive flash cycles are independent and generally not exponentially distributed (being the sum of two independent exponentially distributed random variables with different means). We make no strong assumption about the probability distribution for the escape time $\Theta^{(\mathrm{e})}$ during the last flash cycle, other than that it is essentially independent of the durations $\{\Theta_j^{(\mathrm{f})}\}$ of previous flash cycles.

We claim under these assumptions the holding times should in fact be approximately exponentially distributed and the MCTRW should be a good approximation. (Independence of successive valley jump processes is indicated by the loss of memory

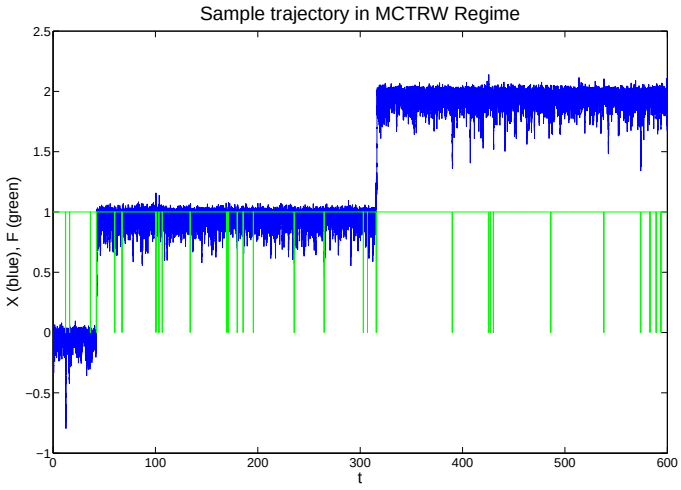


FIG. 5.1. *Depiction of trajectory $X(t)$ of motor particle and state $F(t)$ of flashing potential when MCTRW approximation works well.*

induced by relaxation to local potential minima before escaping). To see this, we express the characteristic function of the holding time $\Theta$

$$\phi_\Theta(k) \equiv \langle \exp(\mathrm{i}k\Theta)\rangle = \left\langle \exp\left( \mathrm{i}k\Big(\sum_{j=1}^{N_F} \Theta_j^{(\mathrm{f})} + \Theta^{(\mathrm{e})}\Big)\right)\right\rangle = G_{N_F}(\phi_{\Theta^{(\mathrm{f})}}(k))\phi_{\Theta^{(\mathrm{e})}}(k)$$

in terms of the characteristic functions of the component times:

$$\phi_{\Theta^{(\mathrm{f})}}(k) = \Big\langle \exp(ik\Theta^{(\mathrm{f})})\Big\rangle, \qquad \phi_{\Theta^{(\mathrm{e})}}(k) = \langle \exp(ik\Theta^{(\mathrm{e})})\rangle,$$

and the probability generating function of the number of flash cycles

$$G_{N_F}(s) = \langle s^{N_F}\rangle.$$

Here we have used standard formulas for the sum of a random number of independent random variables [21, Sec. 1.3]. Now if $N_F$ is geometrically distributed with mean $\bar{N}_F$, then

$$G_{N_F}(s) = \frac{1}{\bar{N}_F(1-s)+1}$$

so

$$\phi_\Theta(k) = \frac{1}{\bar{N}_F(1-\phi_{\Theta^{(\mathrm{f})}}(k))+1}\phi_{\Theta^{(\mathrm{e})}}(k).$$

Now we invoke the assumption that a large number of flash cycles occur between escapes of the particle: $\bar{N}_F \gg 1$. As the mean of the holding time $\Theta$ will scale with $\bar{N}_F$, we need to rescale this random variable accordingly to compute a nontrivial limiting behavior:

$$\tilde{\Theta} \equiv \Theta/\bar{N}_F.$$

The characteristic function of this rescaled random variable, $\phi_{\tilde{\Theta}}(k)$ is obtained from equation (5.1) through

$$\phi_{\tilde{\Theta}}(k) = \phi_{\Theta}(k/\bar{N}_F)$$

so its limiting behavior can be computed as:

$$\begin{aligned}\lim_{\bar{N}_F\to\infty} \phi_{\tilde{\Theta}}(k) &= \lim_{\bar{N}_F\to\infty} \frac{1}{\bar{N}_F(1-\phi_{\Theta^{(\mathrm{f})}}(k/\bar{N}_F))+1}\phi_{\Theta^{(\mathrm{e})}}(k/\bar{N}_F) \\ &= \lim_{\bar{N}_F\to\infty} \frac{1}{\bar{N}_F(1-(1+\mathrm{i}\langle\Theta^{(\mathrm{f})}\rangle k/\bar{N}_F)+1} = \frac{1}{1-ik\langle\Theta^{(\mathrm{f})}\rangle},\end{aligned}$$

which is the characteristic function for an exponentially distributed random variable with mean $\langle\Theta^{(\mathrm{f})}\rangle$. Here we have used the following Taylor expansion for characteristic functions of a general random variable $Y$:

$$\phi_Y(k) = 1 - ik\langle Y\rangle + O(k^2).$$

The limits of characteristic functions imply limits of the corresponding random variables, so we note that $\tilde{\Theta}$ (and therefore the unscaled holding time $\Theta$) has, for large $\bar{N}_F$ (and the other underlying independence assumptions) a probability distribution which is approximately exponentially distributed.

Note that the regime of validity for the MCTRW approximation is not simply the trivial limit in which the potential is turned on most of the time and therefore close to the case of a steady potential.

**5.1. Numerical deterministic calculation of key statistical quantities.** If the times between successive valley visits are not exponentially distributed, then one of the previous assumptions about the picture must fail. We already pointed out that if the holding time $\Theta$ is smaller than or comparable to the relaxation time $\tau^{(\mathrm{rel})} = \alpha^2$, then the picture is invalid and we find no reason to expect the holding times $\{\Theta_j\}$ to be exponentially distributed. This can be quantified through the violation of the self-consistency of the exponential distribution assumption

$$\mathrm{Prob}\{\Theta \le \tau^{(\mathrm{rel})}\} = 1 - \exp(-\tau^{(\mathrm{rel})}/\langle\Theta\rangle) < c, \tag{5.2}$$

where $c$ is a suitably small constant. We also assumed in the above that the relaxation time was short relative to the mean time of a flashing cycle. Violation of this assumption, however, does not appear to destroy Markovianity of the coarse-grained process, provided the relaxation time is short compared to the total holding time. In particular, if we take the extreme limit of a flashing cycle which is very short relative to other time scales, then the motor particle actually feels an effective steady potential equal to $k_{12}^{-1}/(k_{12}^{-1}+k_{21}^{-1})V(x)$, obtained by taking a rapid-fluctuation (annealed) average. Provided that $\theta \ll k_{12}^{-1}/(k_{12}^{-1}+k_{21}^{-1})$ (meaning the flashing potential is not in the off-state for too large a fraction of time), the system behaves effectively like a weakly noisy particle in a steady potential, for which a MCTRW approximation can be expected to hold. Consequently, we don't view the assumption of the relaxation time being short relative to the flash cycle time as vital, and therefore don't consider it further. (The $k_{12} \gg k_{21}$ regime where it becomes an issue will be seen to reside entirely within a regime which can be understood to be non-Markovian through the simpler mechanism described above).

The other key assumption above is that the particle makes a large number of independent escape attempts, meaning the number of flash cycles $N_F$ between jumps to new valleys are typically large. This condition can be formulated as

$$\bar{N}_F \equiv \frac{\langle \Theta \rangle}{\langle \Theta^{(\mathrm{f})} \rangle} = \frac{\bar{\Theta}}{k_{12}^{-1} + k_{21}^{-1}} \gg 1, \tag{5.3}$$

where the expression for $\bar{N}_F$ is an estimate for the typical number of flash cycles per successful escape of the particle.

We now explore how the deviation from the exponential distribution relates to the behavior of the Peclét number for various values of the governing parameters of the flashing ratchet model by computing the coefficient of variation $C_v$ of the holding time $\Theta$:

$$C_v^2 = \frac{\mathrm{var}\,\Theta}{\langle \Theta \rangle^2},$$

which would equal 1 for an exponential distribution. This statistic was analyzed extensively in the context of a static tilted periodic potential by [32]. Another statistical quantity by which we can assess the validity of the MCTRW approximation is through the correlation coefficient of the holding time $\Theta$ and the change in the particle's position $\Xi$ during a given visit between valleys,

$$\rho_{\Xi,\Theta} = \frac{\mathbb{E}[\Xi\Theta] - \Delta\pi \langle \Theta \rangle}{\sqrt{1-\Delta\pi^2}\sqrt{\mathrm{var}\Theta}},$$

where $\Delta\pi = \pi_+ - \pi_-$; this correlation coefficient should vanish for a Markovian continuous-time random walk. Both of these statistical quantities can be computed accurately as solutions of deterministic differential equations arising from the backward-Kolmogorov equation associated to (2.2), as described in Appendix A. We remark here only that the proper calculation does require an auxiliary calculation for the probability distribution of the state of the flashing ratchet at the random moments at which the particle visits a valley; this is not simply the stationary distribution for the flashing ratchet [56, 8]. Moreover these deterministic calculations generate much more accurate results than Monte Carlo simulations, which suffer both from generally slowly decaying sampling error and the need to run simulations for very long times since the transitions between potential minima are relatively rare.

Checking that $C_v \approx 1$ and $\rho_{\Theta,\Xi} \approx 0$ is not strictly sufficient to guarantee the validity of the MCTRW approximation, but are fundamental indicators that are generally violated for processes which are not Markovian continuous-time random walks. Of course we should also check that successive steps are independent; this is not automatic as sometimes assumed [56, 8] because the motor particle trajectory $X(t)$ is not itself Markovian; only the joint process $\{X(t), F(t)\}$ is Markovian. Through selected Monte Carlo simulations, we have found that the correlations between successive steps are generally small. In fact, the correlation coefficients for both holding times $\Theta$ and jump directions $\Xi$ in successive steps were found in all but one simulation to be 0.01 or smaller (within sampling error). The only exception we found was for $k_{12} = 10^{-1.5}$ and $k_{21} = 10^{-0.9}$, the holding times $\Theta$ had correlation coefficient $-0.1 \pm 0.04$, but these parameter values fall in the $C_v > 1$ regime which would already be ruled as non-Markovian. We note that computing these correlations accurately is computationally difficult because have not found a good way to compute these correlations through deterministic equations, as we have done for the statistics $C_v$ and

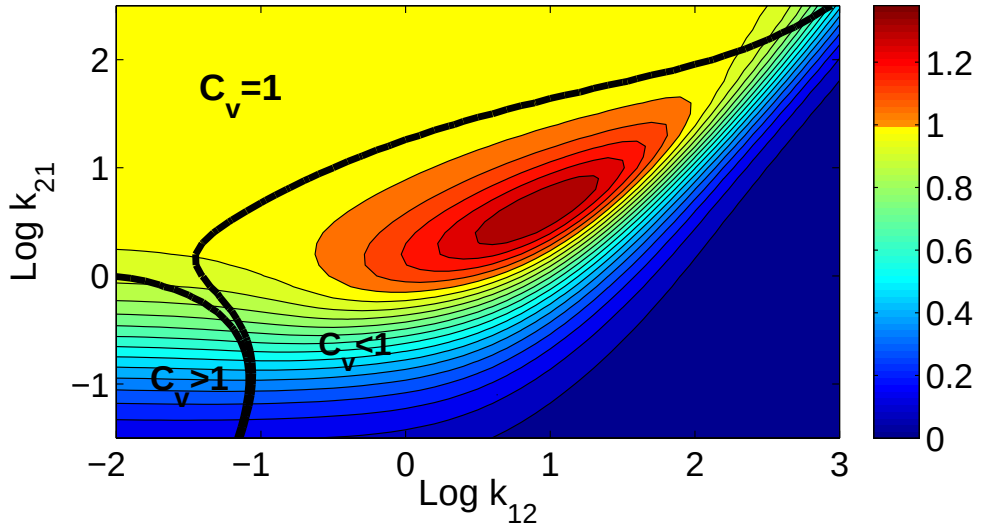


FIG. 5.2. *Level curves of* Pe *as a function of* $k_{12}$ *and* $k_{21}$. ***Black line****: level curves corresponding to* $C_v^2 = 0.99$ *and* $C_v^2 = 1.01$. $\theta = 10^{-1.5}$, $\alpha = 0.85$.

$\rho_{\Theta,\Xi}$, and must therefore resort to Monte Carlo simulations over long enough times to see hundreds to thousands of transitions in order to get even one significant digit of accuracy [27].

In figure 5.2 we have plotted the level curves of the Peclét number as a function of $k_{12}$ and $k_{21}$, as well as the level curves corresponding to $C_v^2 = 0.99$ and $C_v^2 = 1.01$, for $\theta = 10^{-1.5}$. We note the presence of an extensive region where $0.99 < C_v^2 < 1.01$ where the coefficient of variation may be understood to be consistent with that of an exponential distribution. In figure 5.3 we also present $\rho_{\Xi,\Theta}$, which is seen to be relatively small for all parameter values, particularly those corresponding to the $C_v \approx 1$ region in figure 5.2. Taken together with figure 5.2, these figures support our hypothesis that the plateau region in figure 3.2 where $\mathrm{Pe} \approx 1$ corresponds to a region where the continuous dynamics of the flashing ratchet can be approximated by a MCTRW with strong bias. Where the system presents a strong coherence in the transport, characterized by $\mathrm{Pe} > 1$, non-Markovian effects take place ($C_v^2 < 1$).

**5.2. Comparison with theoretical criteria.** As previously discussed, the validity of the MCTRW approximation should only be expected when the escape process behaves as a large number of *failed independent attempts* to escape the potential well before a successful transition. We formulated this condition in terms of the criterion (5.2) that the particle has a small probability to escape a well before relaxing and the criterion (5.3) that the typical number of flashing cycles per successful escape is large. We observe now how these theoretical criteria relate to the numerical results presented above.

In figure 5.4 we have plotted the level curves of $C_v^2$ together with curves delimiting the parameter regions where the theoretical criteria are valid. In so doing, we need to make the inequalities $P(\Theta \leq \tau^{(\mathrm{rel})}) < c$ and $\bar{N}_F \gg 1$ more precise; this is done by noting that specific values for the right hand sides can be found so that the curves so

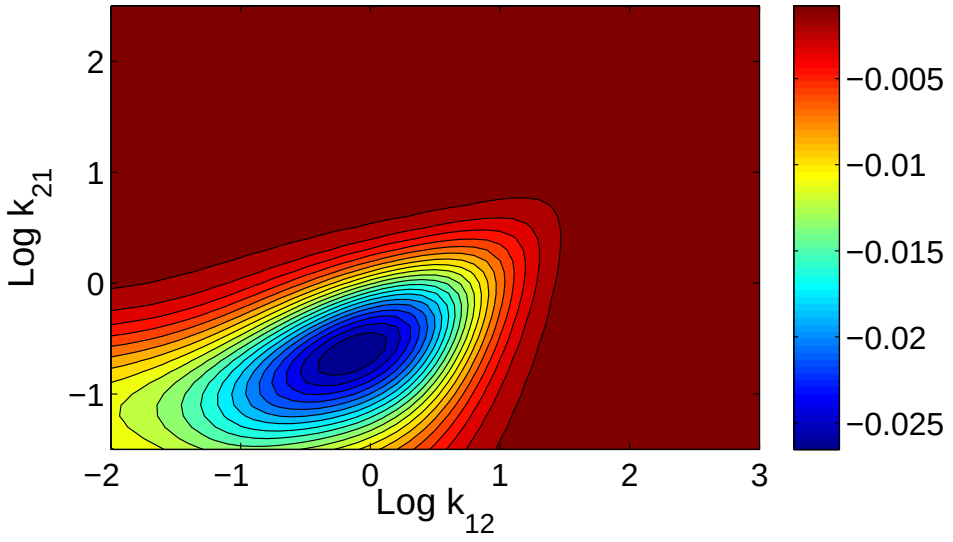


FIG. 5.3. *Level curves of* $\rho_{\Xi,\Theta}$ *as a function of* $k_{12}$ *and* $k_{21}$. $\theta = 10^{-1.5}$, $\alpha = 0.85$.

defined align well with the curves delimiting regimes where the coefficient of variation of the holding time is not close to 1. Note that in each case, we are trying to match a nontrivial curve through one adjustable parameter. We see that the region $C_v = 1$ is very well approximated by the region where $\mathrm{Prob}(\Theta < \tau^{(\mathrm{rel})}) < 0.0035$ and $\bar{N}_F > 5$. The role of the $\bar{N}_F \gg 1$ condition appears somewhat peripheral here, so we also present in figure 5.5 analogous results for a case with higher temperature $\theta = 10^{-1.1}$ (which features a less prominent peak in the Peclét number plot (figure 3.2)).

We further note that the region where $C_v < 1$ appears to correspond to where the particle has a substantial probability of escaping before relaxing to the bottom of the valley of the potential. The $\mathrm{Pe} > 1$ peak in figure 3.2 falls in this regime. A coefficient of variation $C_v < 1$ corresponds to a process which behaves, in a sense, more deterministically than exponential. One well-known mechanism in molecular motor modeling for generating transition times with coefficients of variation below 1 is to introduce several "rate-limiting" steps to the transition process, each with comparable time scales. The resulting time to proceed through such a $m$-step cycle then approximately obeys a Gamma distribution with shape parameter $m$, which has coeffiicent of variation $C_v = 1/m$. Moreover, the Peclét number for such a molecular motor would satisfy $\mathrm{Pe} \approx m$ (often expressed in terms of an equivalent *randomness parameter* $r = 1/\mathrm{Pe}$ [25, 13, 57]. However, here the Peclét number is not close to an integer, so this well-known mechanism is not a good explanation for our observations. However, we might imagine that transitions where the particle does not have time to relax before escaping are governed by some sort of "instanton" process or path of least action [31] which may have a more deterministic character than that corresponding to a large number of independent escape attempts. Indeed, some Monte Carlo simulations of escape time histograms (not shown) indicate that in the $C_v < 1$ regime, the probability distribution for the escape time has a higher probability for a very fast escape relative to the mean than an exponential distribution. Finally,

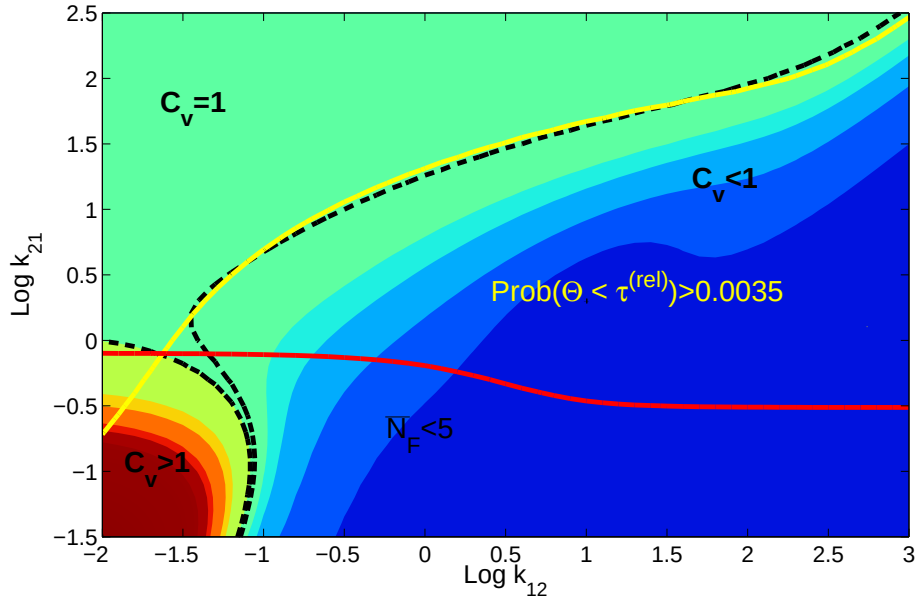


FIG. 5.4. *Level curves of* $C_v^2$ *as a function of* $k_{12}$ *and* $k_{21}$. $\theta = 10^{-1.5}$, $\alpha = 0.85$. ***Yellow:*** $\text{Prob}(\Theta < \tau^{(\text{rel})}) = 0.0035$. ***Red:*** $\bar{N}_F = 5$.

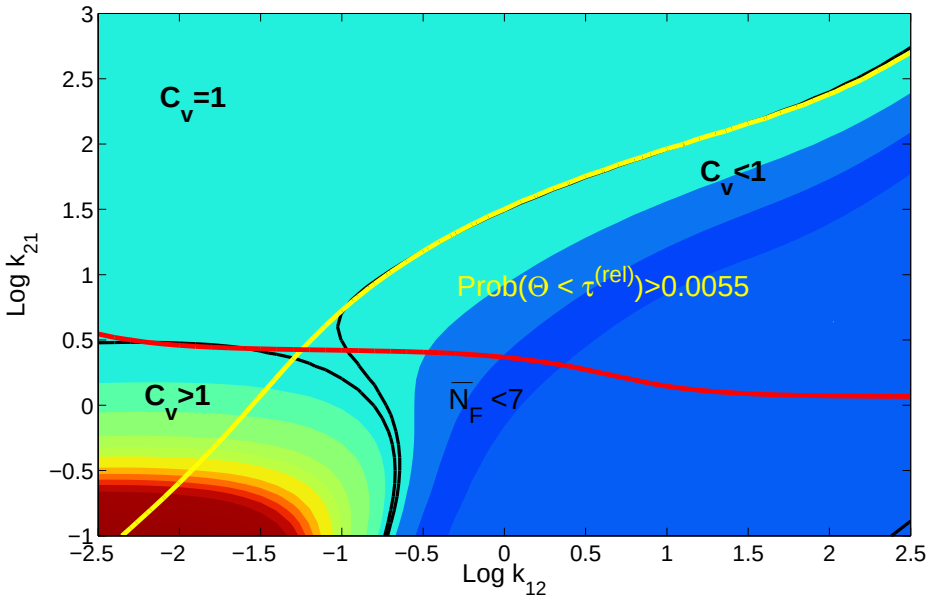


FIG. 5.5. *Level curves of* $C_v^2$ *as a function of* $k_{12}$ *and* $k_{21}$. $\theta = 10^{-1.1}$, $\alpha = 0.85$. ***Yellow:*** $\text{Prob}(\Theta < \tau^{(\text{rel})}) = 0.0055$. ***Red:*** $\bar{N}_F = 7$.

we mention a very interesting self-induced stochastic resonance mechanism described recently [6, 30, 7] for how attaching a massive cargo to a motor can produce nearly deterministic jump times for the motor between potential minima [53]. The coefficient of variation of the jump times $C_v$ in these motor-cargo models is tied to a small parameter characterizing the mobility of the cargo relative to that of the motor [30]. No such asymptotic regime appears relevant in describing the relatively modest reduction in $C_v$ in the simple flashing ratchet models considered here.

Part of the region where the coefficient of variation satisfies $C_v > 1$ appears to be explained by the number of flashing cycles per escape attempt being too small, even though the particle has enough time to relax to the potential minimum between transitions. The time to escape is then governed by the detailed interaction of the particle dynamics and the flashing dynamics; the compounding of the randomness in each of these component processes might explain why the resulting time to escape is more random than an exponential distribution. Monte Carlo simulations of escape time histograms (not shown here) suggest that the time for a fast escape relative to the mean is somewhat suppressed relative to an exponential distribution for the $C_v < 1$ regime.

For parameter values in the lower right of figures 5.4 and 5.5, where both theoretical criteria fail, the resulting coefficient of variation is presumably determined by some suitably weighted superposition of the tendencies for one non-Markovian mechanism to increase the randomness in the escape time and for the other to suppress it.

## 6. Conclusions regarding MCTRW approximation in flashing ratchet model

We have examined the drift and diffusion characteristics of a classical flashing ratchet model and demonstrated at low temperatures that the Peclét number (measuring the coherence, or relative strength of the drift relative to the diffusion) exhibits two noteworthy features as a function of the transition rates of the flashing ratchet. First of all, the Peclét number is approximately one over a wide range of parameters. Secondly, the Peclét number exceeds one over a more limited region, but overlapping the region in which the drift (and therefore utility) of the molecular motor is maximized. We used a Markovian continuous-time random walk (MCTRW) framework in an attempt to understand these observations, together with deterministic equations to compute accurately various statistical quantities which would have required a much greater deal of effort through direct Monte Carlo simulations. We thereby showed that the parameter regime where the Peclét number exhibits a plateau $\mathrm{Pe} \approx 1$ appears to be well modeled by a continuous-time random walk with strong bias. On the other hand, the $\mathrm{Pe} > 1$ region cannot be described by a MCTRW model. We identified two mechanisms by which the MCTRW approximation can be invalidated: the motor particle may escape on a time scale faster than it takes to relax to the minimum of a potential, or the number of flashing cycles per transition of the motor particle from one valley to the next is not large. We showed that the predictions of MCTRW validity by these theoretical criteria are consistent with the numerically computed results. While both mechanisms breaking the MCTRW approximation appear to be operational over parts of the parameter regime, the regime in which drift is optimized seems also to have the property that the motor particle has a substantial probability to escape before it relaxes to the potential minimum.

One central observation, then, is that the simple characterization of a molecular motor's progress as a Markovian continuous-time random walk between valleys is

not necessarily appropriate for the regime in which the molecular motor generates the fastest transport. One can of course turn to generalized random walk models in which the time between transitions has a general (not necessarily exponential) probability distribution, but each transition proceeds independently of other transitions. That is, the flashing ratchet model might be accurately coarse-grained as a renewal process [21, Ch. 5] where memory is lost only at the special (random) moments when a new valley is visited, rather than the fully Markovian classical continuous-time random walk models which at any time carries no memory other than its current state (and therefore must have an exponential distribution between visits to successive states [21, Sec. 4.2]).

**7. Parameterization of dynamics of water molecules near solute**

We next turn to our second molecular biology model, which concerns the statistical parameterization of the dynamics of water molecules near a solute. Though our eventual interest is the behavior of water near proteins, here we use a very simplified setting to gain insight into some of the mathematical issues in play. We choose a $C_{60}$ buckyball consisting of 60 carbon atoms distributed approximately symmetrically about a sphere. The chemical homogeneity and approximate isotropy imply that the behavior of water molecules should be purely a function of distance from the center of the buckyball. In figure 1.1 we show a snapshot of a molecular dynamics simulation [54, 14], conducted by Shekhar Garde's research group, of a buckyball with 4200 "simple point charge" surrounding water molecules. The computational details for the simulation are similar to those used in [20] for hydrated carbon nanotube simulations. Our main interest will be to obtain a useful statistical parameterization of the dynamics of the water molecules in this detailed molecular dynamics simulation.

The first question to be addressed is the framework in which the statistical dynamics of the water molecules are to be quantified. One measure which can be found in the biophysical literature is the following generalization of a diffusion tensor, which we will call the "biophysical diffusivity" [37, 34]:

$$D_B(\boldsymbol{r}) \equiv \left\langle \frac{|\boldsymbol{X}(t+2\tau)-\boldsymbol{X}(t)|^2}{6\tau} - \frac{|\boldsymbol{X}(t+\tau)-\boldsymbol{X}(t)|^2}{6\tau} \,\middle|\, \boldsymbol{X}(t)=\boldsymbol{r} \right\rangle. \tag{7.1}$$

Here the angle brackets $\langle\cdot|\cdot\rangle$ denote a conditional statistical average of the quantity to the left of the bar, given the condition to the right of the bar. In practice, such a statistical average is obtained by dividing space into bins (which for the present case would typically be spherical shells), running a long molecular dynamics simulation, sorting the data about the increments $\boldsymbol{X}(t+2\tau)-\boldsymbol{X}(t)$ and $\boldsymbol{X}(t+\tau)-\boldsymbol{X}(t)$ based on the location $\boldsymbol{X}(t)$ of the water molecule at the beginning of the time increment, and then taking the conditional statistical average (7.1) over the data over all water molecules and time instants $t$ for which $\boldsymbol{X}(t)$ fell within the bin under consideration. The time increment $\tau$ is supposed to be long compared to the momentum relaxation time of the water molecule, but short enough so that the water molecule does not move far from the shell in which it started at the beginning of the time interval $[t,t+2\tau]$ of interest. In practice, a value of $\tau=1$ ps $(=10^{-12}$ s) is typically chosen. Note that the diffusivity $D_B(\boldsymbol{r})$ is assumed not to depend on $t$ because data is understood to be taken only once the system has adequately achieved thermal equilibrium; this is what allows data from different moments of time to be pooled in the numerical computation of the statistical average (and thereby to have any hope of achieving adequate statistics).

The details of the expression (7.1) may be a bit difficult to parse, but one may observe that in a bulk water environment away from any solute or disturbance which creates a bias or spatial dependence on the statistical dynamics of the water molecules, the expression (7.1) agrees with the traditional measure of diffusivity,

$$D_0 = \left\langle \frac{|\boldsymbol{X}(t+\tau)-\boldsymbol{X}(t)|^2}{6\tau} \right\rangle,$$

where $\tau$ is any time increment large compared to the momentum relaxation time of the water molecule, so that over the time increment $[t,t+\tau]$ the water molecule behaves diffusively rather than inertially [44]. Note in particular that the bulk diffusivity should be approximately independent of $\tau$ once this condition is met.

The diffusivity measure (7.1) does show interesting variations from the bulk diffusivity value as the location $\boldsymbol{r}$ of the water molecule approaches the solute [37, 34], but yet one may ask how informative this measure is. One might argue as well that the dynamics of water molecules may behave differently in the direction approaching the solute surface as compared to the directions parallel to the solute's nearest surface. Such anisotropy in the statistics of the water molecule dynamics has indeed been adequately appreciated in the literature, and the definition (7.1) for the local difffusivity has been generalized in these terms [37]. Of greater concern to the present discussion, the quantity (7.1) (as well as its anisotropic generalizations) seems to mix together both bias in the dynamics of water molecules as well as changes in the random component of its mobility. The mathematical theory of diffusion processes [24, Sec. 1.7] offers what appears to be a more natural decomposition of the local behavior of water molecules near a solute in terms of a deterministic bias and a random motion. Specifically, we define a drift coefficient

$$\boldsymbol{U}(\boldsymbol{r},\tau) \equiv \left\langle \frac{\boldsymbol{X}(t+\tau)-\boldsymbol{X}(t)}{\tau} \middle| \boldsymbol{X}(t)=\boldsymbol{r} \right\rangle \tag{7.2a}$$

to capture the deterministic bias and the diffusion tensor

$$\mathsf{D}(\boldsymbol{r},\tau) \equiv \left\langle \frac{(\boldsymbol{X}(t+\tau)-\boldsymbol{X}(t)-\boldsymbol{U}(\boldsymbol{r})\tau)\otimes(\boldsymbol{X}(t+\tau)-\boldsymbol{X}(t)-\boldsymbol{U}(\boldsymbol{r})\tau)}{2\tau} \middle| \boldsymbol{X}(t)=\boldsymbol{r} \right\rangle \tag{7.2b}$$

to quantify the strength of the unpredictable component of the water molecules along various directions, as observed over a time scale $\tau$. For theoretical purposes, the $\tau \to 0$ limit is taken, but in working with practical data we must keep $\tau$ finite. We note that the terms $\boldsymbol{U}(\boldsymbol{r})\tau$ are usually omitted in the definition of the diffusion tensor in the mathematical theory of diffusion processes [24, Sec. 1.7] but it makes no change in the $\tau \to 0$ limit and clarifies the intended decomposition for practical implementation with finite $\tau$.

For the case of a spherically symmetric solute (a property satisfied approximately by the $C_{60}$ buckyball), the drift vector and diffusion tensor in fact can be represented in terms of three scalar functions as follows:

- $\boldsymbol{U}(\boldsymbol{r},\tau) = U_{\parallel}(|\boldsymbol{r}|,\tau)\hat{\boldsymbol{r}}$,
- $\mathsf{D}(\boldsymbol{r},\tau) = D_{\parallel}(|\boldsymbol{r}|,\tau)\hat{\boldsymbol{r}}\otimes\hat{\boldsymbol{r}} + D_{\perp}(|\boldsymbol{r}|,\tau)(\mathsf{I}-\hat{\boldsymbol{r}}\otimes\hat{\boldsymbol{r}})$,

where $\hat{\boldsymbol{r}} = \boldsymbol{r}/|\boldsymbol{r}|$ and $\mathsf{I}$ is the identity matrix. That is, the drift can only be directed toward or away from the solute, with magnitude and sign depending only on the distance from the center of the solute:

$$U_{\parallel}(|\boldsymbol{r}|,\tau) = \left\langle \frac{\boldsymbol{X}(t+\tau)-\boldsymbol{X}(t)}{\tau}\cdot\hat{\boldsymbol{r}} \middle| \boldsymbol{X}(t)=\boldsymbol{r} \right\rangle.$$

The random component of the motion is expressed in terms of a longitudinal diffusivity

$$D_{\parallel}(|\boldsymbol{r}|,\tau) = \left\langle \frac{\left|(\boldsymbol{X}(t+\tau)-\boldsymbol{X}(t))\cdot\hat{\boldsymbol{r}} - U_{\parallel}(\boldsymbol{r})\tau\right|^2}{2\tau} \middle| \boldsymbol{X}(t)=\boldsymbol{r} \right\rangle,$$

which describes the vigor of the random motion toward and away from the solute, and the lateral diffusivity

$$D_{\perp}(|\boldsymbol{r}|,\tau) = \left\langle \frac{1}{4\tau}\left|(\boldsymbol{X}(t+\tau)-\boldsymbol{X}(t))\cdot(\mathsf{I}-\hat{\boldsymbol{r}}\otimes\hat{\boldsymbol{r}})\right|^2 \middle| \boldsymbol{X}(t)=\boldsymbol{r} \right\rangle,$$

which describes the vigor of the random motion parallel to the nearest solute surface (which here means along the angular directions with respect to the center of the solute).

One useful property of the drift and diffusion coefficients described above is that models or estimations for these quantities immediately can be used to define a complete stochastic model for the dynamics of the center of mass of a water molecule through the following stochastic differential equation

$$\mathrm{d}\boldsymbol{X} = \boldsymbol{U}(\boldsymbol{X}(t),\tau)\,\mathrm{d}t + \Sigma(\boldsymbol{X}(t),\tau)\,\mathrm{d}\boldsymbol{W}(t), \tag{7.3}$$

where $\mathrm{d}\boldsymbol{W}(t)$ is a stochastic increment of Brownian motion (or the Wiener process), which formally may be treated as a mean zero Gaussian random vector with covariance $\langle(\mathrm{d}W_i(t)\mathrm{d}W_j(t))^2\rangle = \delta_{ij}\mathrm{d}t$ (with $\delta_{ij}=1$ for $i=j$ and vanishes otherwise), and stochastic increments at different times are independent [15, Ch. 4]. $\Sigma(\boldsymbol{r},\tau)$ is obtained through a matrix square-root of the positive definite diffusion tensor:

$$\mathsf{D}(\boldsymbol{r},\tau) = \frac{1}{2}\Sigma(\boldsymbol{r},\tau)\Sigma^{\dagger}(\boldsymbol{r},\tau).$$

$\Sigma(\boldsymbol{r},\tau)$ is not uniquely defined by this relationship, but any solution can be shown to generate a stochastic model equivalent to any other choice. In the isotropic case, the noise coefficient can be simply expressed as

$$\Sigma(\boldsymbol{r},\tau) = \sqrt{2D_{\parallel}(\boldsymbol{r},\tau)}\hat{\boldsymbol{r}}\otimes\hat{\boldsymbol{r}} + \sqrt{2D_{\perp}(\boldsymbol{r},\tau)}(\mathsf{I}-\hat{\boldsymbol{r}}\otimes\hat{\boldsymbol{r}}).$$

Particle trajectories generated by the drift-diffusion model (7.3) using an Euler-Marayama discretization [24, Sec. 9.1] with time step $\Delta t=\tau$ would self-consistently produce drift and diffusion coefficients (7.2) equal to those used in defining the model, but the stochastic differential Equ. (7.3) also makes sense as a continuous-time model (which could be simulated with time steps $\Delta t\neq\tau$).

**8. Parameterization of drift-diffusion model**

We now examine the mathematical definitions of drift and diffusivity (7.2) as a basis for parameterizing these coefficients directly from a molecular dynamics simulation. As elaborated in [47, 46, 42], such a parameterization of coarse-scale coefficients in a multiscale system is not entirely straightforward. The essential question of interest to us here is the choice of time increment $\tau$ used to evaluate the drift and diffusion coefficients in (7.2). Once $\tau$ has been chosen, the calculation of the statistical estimates for these coefficients can be achieved through collecting data from a suitably long time series of a simulation with many water molecules and evaluating the conditional average through sorting the data of the time increments into spatial

bins (here spherical shells) as described after equation (7.1) above. Now, the mathematical definitions (7.2) indicate that the limit $\tau \downarrow 0$ is desired, which might suggest that $\tau$ be chosen equal to the time step $\Delta t$ used in the molecular dynamics simulations. However, as is well recognized in the literature, the diffusion coefficient will not be correctly estimated unless the time increment $\tau$ is chosen to be long compared to the momentum relaxation time $T_V$ of the water molecules. Indeed, the description of the motion of a water molecule in bulk as thermal Brownian motion (that is through a stochastic differential equation (7.3) with $\boldsymbol{U} \equiv \boldsymbol{0}$ and $\Sigma = \sqrt{2D_0}\mathsf{I}$) is valid only over such relatively coarse time scales $\tau \gg T_V$; on shorter time scales something like a Langevin equation explicitly involving the velocity variable of the water molecule is required [5]. In practice, then, diffusivities of water molecules in molecular dynamics simulations are calculated through statistics of displacements over time increments $\tau \gtrsim 0.2$ ps $(= 0.2 \times 10^{-12}$ s) [51].

One might simply proceed to use this same value of $\tau$ for our drift-diffusive parameterization near a solute, but a few complicating factors raise some concerns. First of all, the inhomogeneity induced by the solute may affect the momentum relaxation time scale $T_V$ significantly. More importantly, an inhomogenous environment imposes upper limits $T_X$ on $\tau$ so that the particle is not wandering far from the bin associated to its value $\boldsymbol{X}(t)$ at the beginning of the time interval $[t, \tau]$. Otherwise, the statistics collected for the drift coefficient $\boldsymbol{U}(\boldsymbol{r})$ and diffusion coefficient $\mathsf{D}(\boldsymbol{r})$ do not really describe the local behavior at the position $\boldsymbol{r}$. In bulk, the upper limit on $\tau$ is much more generous – the particles essentially should not move a distance comparable to the size of the domain (periodic or confining) over a time interval of length $\tau$. One may be concerned that the value $\tau \gtrsim 0.2$ ps chosen for calculating water diffusivity in bulk may not be an optimal or even appropriate choice to describe water molecule dynamics near the surface of a solute, where we seek $T_V \ll \tau \ll T_X$, where the momentum and position time scales $T_V$ and $T_X$ may themselves depend significantly on position [52].

To illustrate and gain insight into this issue, we first examine it in the context of a greatly simplified, exactly solvable model, and the consider what lessons from the exactly solvable model might be transferable to the parameterization of the more complex buckyball system in which we are interested.

## 9. Toy model for drift-diffusion parameterization

Consider the following simple Ornstein-Uhlenbeck model for the dynamics of a particle:

$$\begin{aligned} \mathrm{d}\boldsymbol{X} &= \boldsymbol{V}\,\mathrm{d}t, \\ m\mathrm{d}\boldsymbol{V} &= -\gamma \boldsymbol{V}\,\mathrm{d}t - \alpha \boldsymbol{X}\,\mathrm{d}t + \sqrt{2k_B T\gamma}\,\mathrm{d}\boldsymbol{W}(t). \end{aligned} \tag{9.1}$$

Here $\boldsymbol{X}$ denotes the particle position, $\boldsymbol{V}$ the particle velocity, $m$ the particle mass, and $\gamma$ the friction coefficient of the particle. These equations describe dynamics according to Newton's law with a friction force $-\gamma \boldsymbol{V}$ and harmonic potential $\frac{1}{2}\alpha|\boldsymbol{r}|^2$. The conceptual simplifications of this simple model relative to the true equations of motion for a water molecule in the molecular dynamics simulations is that the complicated effective potential acting on a water molecule through the combination of the solute and other water molecules is replaced by a harmonic potential, and the interactions with other water molecules are replaced by standard Langevin-type friction and noise terms. We nondimensionalize the equations (9.1) with respect to

spatial scale $\sqrt{k_BT/\alpha}$ and time scale $T_X=\gamma/\alpha$ to obtain

$$\begin{aligned}\mathrm{d}\boldsymbol{X}&=\boldsymbol{V}\,\mathrm{d}t,\\ \mathrm{d}\boldsymbol{V}&=-a\boldsymbol{V}\,\mathrm{d}t-a\boldsymbol{X}\,\mathrm{d}t+a\,\mathrm{d}\boldsymbol{W}(t),\end{aligned}\tag{9.2}$$

where $a=\gamma^2/(m\alpha)$ is the ratio of the position time scale $T_X$ to the momentum time scale $T_V=m/\gamma$. Now, in the limit $a\to\infty$ this system of equations can be shown through standard Smoluchowski reduction [15, Sec. 6.4] to be well approximated by the reduced system

$$\mathrm{d}\boldsymbol{X}=-\boldsymbol{X}\,\mathrm{d}t+\mathrm{d}\boldsymbol{W}(t),\tag{9.3}$$

which we see is of drift-diffusion type for the variable $\boldsymbol{X}$ with drift $\boldsymbol{U}(\boldsymbol{r})=-\boldsymbol{r}$ and diffusion tensor $\mathsf{D}(\boldsymbol{r})=\frac{1}{2}\mathsf{I}$.

Now suppose that (as will be the case in practical systems) we do not know how to derive this analytical reduction, but rather need to estimate $\boldsymbol{U}(\boldsymbol{r})$ and $\mathsf{D}(\boldsymbol{r})$ through collecting data from trajectories simulated by the full system (9.2) for some large but finite value of $a$ and computing conditional averages (7.2) with some choice of time increment $\tau$. The question we will pose is what choice of $\tau$ gives the best agreement with the exact asymptotic results (9.2).

We will put aside questions of spatial binning and statistical sampling by using the exact solution to (9.2):

$$\begin{aligned}\boldsymbol{X}(t)=&\frac{\alpha_2\mathrm{e}^{-\alpha_1 t}-\alpha_1\mathrm{e}^{-\alpha_2 t}}{\alpha_2-\alpha_1}\boldsymbol{X}(0)+\frac{\mathrm{e}^{-\alpha_1 t}-\mathrm{e}^{-\alpha_2 t}}{\alpha_2-\alpha_1}\boldsymbol{V}(0)\\&+\frac{\alpha_1\alpha_2}{\alpha_2-\alpha_1}\int_0^t\left(\mathrm{e}^{-\alpha_1(t-s)}-\mathrm{e}^{-\alpha_2(t-s)}\right)\mathrm{d}\boldsymbol{W}(s)\end{aligned}$$

where $\alpha_1=\frac{a-\sqrt{a^2-4a}}{2}$ and $\alpha_2=\frac{a+\sqrt{a^2-4a}}{2}$. This allows all the conditional averages in (7.2) to be calculated exactly for arbitrary values of $\tau$.

We obtain in this way

$$\begin{aligned}U_\parallel(r,\tau)&=\frac{\left[\frac{1}{\alpha_2-\alpha_1}\left(\alpha_2\mathrm{e}^{-\alpha_1\tau}-\alpha_1\mathrm{e}^{-\alpha_2\tau}\right)-1\right]}{\tau}r,\\ D_\parallel(r,\tau)&=D_\perp(r,\tau)\\&=\left(\frac{\alpha_1\alpha_2}{\alpha_2-\alpha_1}\right)^2\frac{\frac{1}{2\alpha_1}\left(1-\mathrm{e}^{-2\alpha_1\tau}\right)-\frac{2}{\alpha_1+\alpha_2}\left(1-\mathrm{e}^{-(\alpha_1+\alpha_2)\tau}\right)+\frac{1}{2\alpha_2}\left(1-\mathrm{e}^{-2\alpha_2\tau}\right)}{2\tau}.\end{aligned}$$

These formulas are most usefully interpreted through their graphs in figure 9.1.

We observe that indeed the values of $\tau$ which produce effective drift and diffusion coefficients close to the desired values fall in an intermediate range of times. In fact, the values of $\tau$ which give closest agreement to the rigorous asymptotic value can be shown to scale as the geometric mean of the position time scale $T_X\sim 1$ and momentum relaxation time scale $T_V\sim 1/a$ and therefore in particular satisfy $T_V\ll\tau\ll T_X$ for large $a$. We also see that the effective drift and diffusivity never actually achieve the $a=\infty$ asymptotic value for any value of $\tau$, but this simply reflects the fact that $a$ is large but finite. (The drift and diffusivity values chosen at the optimal value of $\tau$ at finite $a$ depart from the $a=\infty$ asymptotics (9.3) by terms proportional to $a^{-1/2}$). So we are more precisely looking for a way of choosing values of $\tau$ such that as $a\to\infty$,

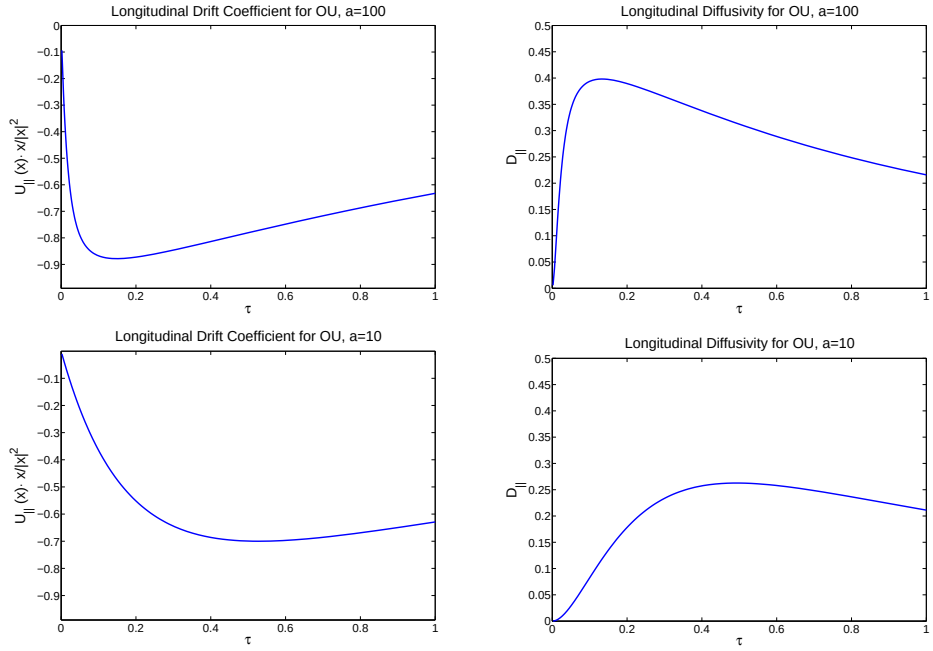


FIG. 9.1. *Longitudinal drift (left) and longitudinal diffusivity (right) for the Ornstein-Uhlenbeck model (9.2) as computed with different sampling time intervals $\tau$. The lateral diffusivity equals the longitudinal diffusivity in this model.*

the drift and diffusivities computed by the conditional averages (7.2) converge to the asymptotic results corresponding to the rigorous coarse-graining.

Now in the more complex setting of water molecules near a solute, we cannot really expect to transfer the details of these results because they are probably not robust under the change in potential and we cannot really estimate $T_V$ and $T_X$ so precisely. But a softer observation does seem to have promise of useful generalization: the best values of $\tau$ for estimating the drift and diffusivity appear to be those for which those values are most pronounced (relative to those obtained from other values of $\tau$). Choosing $\tau$ too large or too small seems to wash out the computed conditional averages (7.2). This can be understood as follows: For small $\tau$ (particularly $\tau \lesssim 1/a$), the dynamics of the particle velocity are being resolved enough that $\boldsymbol{V}(t)$ does not behave like approximate white noise superposed on an offset depending on $\boldsymbol{X}$ (as must be the case if equation (9.3) is to approximate equation (9.2)). Indeed, for $\tau \ll 1/a$, we can write $\boldsymbol{X}(t+\tau)-\boldsymbol{X}(t) \sim \boldsymbol{V}(t)\tau + O(a^{3/2}\tau^2)$, in which case $\boldsymbol{U}(\boldsymbol{r},\tau) \sim \langle \boldsymbol{V}(t)|\boldsymbol{X}(t)=\boldsymbol{r}\rangle + O(a\tau) = O(a\tau)$ (where we have noted that the $O(a^{3/2}\tau)$ part of the error has mean zero) and $\mathsf{D}(\boldsymbol{r},\tau) \sim \frac{1}{2}\langle \boldsymbol{V}(t)\otimes\boldsymbol{V}(t)|\boldsymbol{X}(t)=\boldsymbol{r}\rangle\tau + O(a^2\tau^2) = \frac{a\tau}{4}\mathsf{I} + O(a^2\tau^2)$. That is, both the computed drift and diffusivity vanish with $a\tau$. On the other hand, for $\tau \gtrsim 1$, the particle is moving by an $O(1)$ amount during the time interval $[t,t+\tau]$ and is therefore not really sampling local dynamical behavior near a particular position $\boldsymbol{r}$. Indeed, for $\tau \gg 1$, the conditional averages would approximate the global drift and diffusion coefficient (describing the long time asymptotics of the particle displacement) which here are both zero because of the confining potential.

We hypothesize that this general property of the best value of $\tau$ being that which

gives a most pronounced conditional average (7.2) for the drift and diffusivity carries over to more realistic systems such as the buckyball under consideration. One distinction that may call this into question is that the real potential of interaction between the water molecule and solute will be multiwelled and decaying toward zero at large distances (figure 9.2), rather than having a simple harmonic form. This doesn't greatly affect the conclusions about small $\tau$ but may affect those concerning large $\tau$ which appealed to the global drift and diffusivity of the simple system (9.2) being zero. The global drift can also be expected to be zero in the buckyball system as a consequence of thermal equilibrium, but the global diffusivity should be expected to be a finite nonzero constant, somewhat altered from the bulk diffusivity value by the trapping and repelling effects of the buckyball.

This motivates the following scheme for choosing the value of $\tau$ for computing the conditional averages in the buckyball system. We first seek a rough estimate based on a crude transferral of results from the Ornstein-Uhlenbeck system (9.1). To do so, we need to relate parameters of the Ornstein-Uhlenbeck system to that of the molecular dynamics simulation. The parameter $\alpha$ defining the harmonic potential in the toy model will require the most explanation. We begin by introducing the notion of the *potential of mean force* $\phi(\boldsymbol{r})$, defined in terms of the concentration $c(\boldsymbol{r})$ of the water molecules in thermal equilibrium

$$\phi(\boldsymbol{r}) = -k_B T \ln(c(\boldsymbol{r})/c_0),$$

where $k_B$ is Boltzmann's constant and $c_0$ is the average concentration of water molecules (total number divided by total volume of system). This choice produces a Boltzmann-type distribution for the water molecule concentration:

$$c(\boldsymbol{r}) \propto \mathrm{e}^{-\phi(\boldsymbol{r})/(k_B T)}.$$

The idea is that the mean motion of the water molecule is like overdamped motion in an effective potential. The potential of mean force is like a free energy in that it takes into account not only the forces between the solute and the water molecule under consideration, which are well specified because each are at known locations, but also all the forces induced by the presence of other water molecules, with locations not explicitly specified and therefore effectively averaged over in a self-consistent statistical sense. Because this statistical averaging over all the other water molecules requires an accurate representation of joint multiparticle statistics, it is extremely difficult to compute theoretically (see [39] for some techniques involving analytical approximations). We therefore will extract data from molecular dynamics simulations to estimate $c(\boldsymbol{r})$; this is a routine task of simply binning up space (in the current isotropic case into radial shells) and counting at each time step how many water molecules are in each bin, and then averaging over time (once thermal equilibrium is achieved.) The binned results are smoothed using a 7-hat filter, meaning that each binned value is replaced by its average over a centered window of width equal to 7 bins. The resulting potential of mean force (which here is radial $\phi = \phi(r)$) and its derivative are shown in figure 9.2. The oscillations arise entirely from collective effects of the water molecules — the direct interaction between the carbon atoms of the buckyball and a given water molecule is of a simple Lennard-Jones form [14] with a repulsive core and attractive tail. The oscillations reflect the tendency for the water molecules to be located in hydration shells of roughly multiples of 0.2–0.3 nm from the surface of the solute [29]).

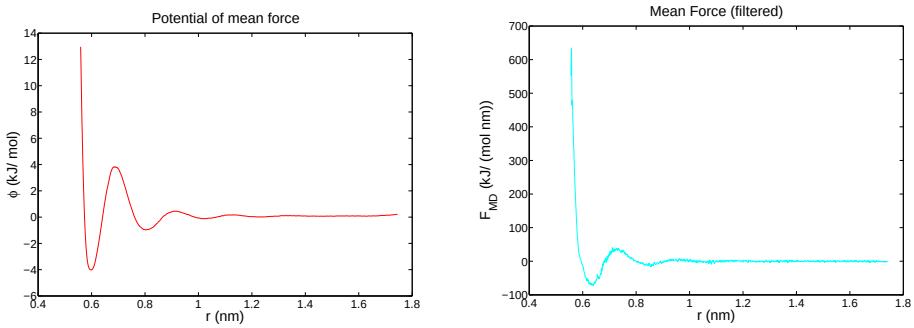


FIG. 9.2. *Potential of mean force for the buckyball (left) and mean force (right).*

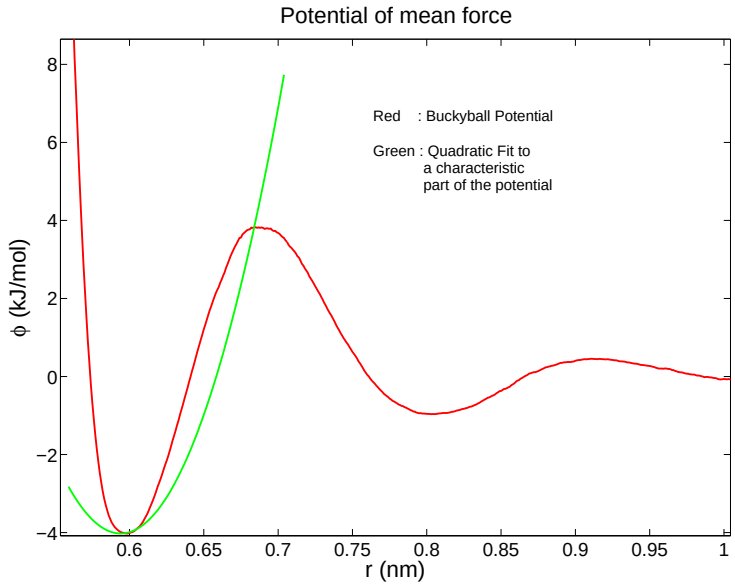


FIG. 9.3. *Quadratic fit to the first hydration shell of the buckyball potential*

With the potential of mean force now playing the role of the effective potential felt by a water molecule, we associate to it a value $\alpha = 1500 \frac{\text{kJ}}{\text{mol nm}^2}$ by fitting a parabola to the first hydration shell (figure 9.3). Of course this is not to say the potential of mean force is approximately harmonic, but simply that for the purposes of estimating the time scale on which the position of a water molecule is induced to fluctuate, we take this value of $\alpha$ to characterize the order of magnitude of the curvature of the potential.

The other parameters in the associated Ornstein-Uhlenbeck model can be more straightforwardly quantified by basic physical considerations. We take the mass $m = 18.2 \times 10^{-24}$ g of a water molecule, and set $\gamma = 6.8 \times 10^{-10}$ g/s by using the Einstein relation $D_0 = \frac{k_B T}{\gamma}$, $k_B T = 2.3 \frac{\text{kJ}}{\text{mol}}$ for a physiological system, and $D_0 = 0.0056 \frac{\text{nm}^2}{\text{ps}}$ from the MD simulations. This yields a momentum relaxation time scale $T_V = 27\text{fs} =$

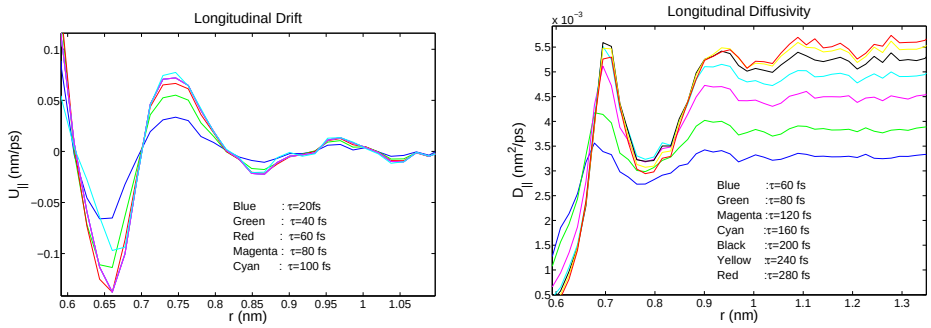


FIG. 9.4. *Longitudinal drift and diffusivity plots obtained from MD data for the buckyball for various choices of sampling time interval* $\tau$.

0.027 ps for the water molecule. Note how the usual choice of 0.2 ps as the time scale for computing the diffusivity of water molecules (in bulk) is a few multiples of this time scale. Next, we estimate the value of the nondimensional parameter $a$ describing the ratio of the time scales of the position and the velocity of the water molecule using the formula $a = \frac{m\gamma^2}{\alpha}$ and obtain $a = 10$, a reasonably but not enormously large value. This indicates the need for some care in finding time increments $\tau$ satisfying the desired conditions $T_V \ll \tau \ll T_X$ (see figure 9.1).

We take as a rough initial guess $\tau \approx T_V a^{1/2} = 85$ fs as suggested by the harmonic model. But more importantly, we vary $\tau$ around this value and look to find where the conditional averages (7.2) are most pronounced. The results are displayed in figure 9.4; these graphs are of course more complicated than those appearing in figure 9.1 because the spatial dependence is now nontrivial. The numerical observations appear to confirm the hypotheses inferred from the Ornstein-Uhlenbeck model. The conditional averages for the drift give a more pronounced result as $\tau$ increases from 20 to 80 fs, and then washes out as $\tau$ is increased further. On the other hand, we see that the conditional averages defining the effective diffusivity increase significantly with $\tau$ until $\tau \approx 200$ fs, after which the conditional averages seem to saturate approximately. We could continue to even larger values of $\tau$ to see if the structure of the diffusivity coefficient degrades, but there is not much point in doing so because 200 fs is already quite a bit larger than the value of 80 fs for which the drift coefficient was most pronounced. Apparently, the best values of $\tau$ for representing the drift and the best values of $\tau$ for representing the diffusivity do not really overlap, as they did for the simple Ornstein-Uhlenbeck model. A similar phenomenon in simultaneuous parameter estimation through sampling of time series was found in related mathematical multiscale models [47, 46, 42]. This can perhaps be understood as follows: as discussed above the diffusivity can only be estimated properly, even in bulk, by considering the statistics of increments over time intervals sufficiently long relative to the momentum decorrelation time $T_V \sim 27$ fs. From figure 9.4, this constraint appears to be $\tau \gtrsim 200$ fs, which is consistent with the commonly used criterion in molecular dynamics [51]. On the other hand, the time scale of the position of the water molecule is naturally affected by the potential of mean force, and one constraint for example should be that the water molecule cannot move from the bottom of the potential in the first hydration shell over the barrier to the second hydration shell over a time $\tau$. This time scale may be estimated as the position time scale $T_X \sim 270$ fs – so the

desired condition $T_V \ll \tau \ll T_X$ may not be realizable in a strong sense in practice (given that $T_X/T_V = a = 10$ is not that large).

The idea of using different values of $\tau$ to estimate the drift and diffusion coefficient is numerically inconsistent because then equation (7.3) would refer to coarse-grained coefficients over two different time scales. One can see the problem by starting with a stochastic differential equation of the form (7.3) and coarse-graining it by leaving the drift or diffusion coefficient fixed (corresponding to a coarse-graining over a very small time scale $\tau$) while replacing the other coefficient by a coarse-grained conditional average (7.2) obtained from trajectories of the original system. The resulting stochastic differential equation which retains one coefficient from the original system but has replaced the other by some "coarse-grained" value does not approximate the original stochastic differential equation in any meaningful way. At least choosing a common value of $\tau$ to coarse-grain both the drift and diffusion coefficient ensures that when the coarse-grained stochastic model (7.3) is integrated using an Euler-Marayama scheme [24, Sec. 9.1] with time step $\tau$, then the conditional averages (7.2) obtained from the coarse-grained model (for this selected value of $\tau$) will agree with those obtained from the full molecular dynamics simulation.

For these reasons, we choose $\tau = 200$ fs to parameterize the drift and diffusion coefficients by the conditional averages (7.2). The reason is that 200 fs seems to be a minimal value to obtain a reasonable behavior for the diffusivity coefficient. Particularly the bulk value (at large $r$) is an essential transport property which must be represented properly in the coarse-grained model. On the other hand the best value of $\tau$ for computing the drift coefficient appears to be approximately 80 fs, and degrades for larger values of $\tau$. The value of 200 fs approximately meets the requisites for satisfactory estimation of the diffusivity coefficient, and is as close as possible to the optimal values of $\tau$ for estimating the drift.

The drift and diffusivity coefficients obtained with $\tau = 200$ fs are presented in figure 9.5. The deterministic component (effective drift) of the motion might be expected to be essentially proportional to the mean force in figure 9.2 because the water molecule dynamics are overdamped, and we see this to be at least qualitatively the case. We observe similar oscillations reflecting the hydration shell structure in the longitudinal diffusivity, but not in the lateral diffusivity. Both the longitudinal and lateral diffusivity are suppressed near the buckyball surface (approximately 0.6 nm from the center).

**10. Conclusions regarding drift-diffusion parameterization model for water molecule dynamics**

We have sought to model the drift and diffusion coefficients in the stochastic model (7.3) in the most accurate manner possible — the extraction of statistics from data obtained from detailed molecular dynamics simulations. This may raise the question of the purpose of this exercise, since the coarse-grained model (7.3) is supposed to permit simulation of the water molecule dynamics without requiring expensive detailed simulations. One way in which such a data-driven parameterization can be useful in predictive modeling is that the detailed molecular dynamics data is obtained from some studies in some representative simplified settings (near solutes of particular topologies and chemistries) and these results then assembled into predictive stochastic models for the water molecules near new solutes and proteins composed of structures similar to those from which the detailed molecular dynamics simulations were conducted. In some sense, this is conceptually like the parameterization of atomic force fields in the molecular dynamics simulation codes themselves, which are obtained from

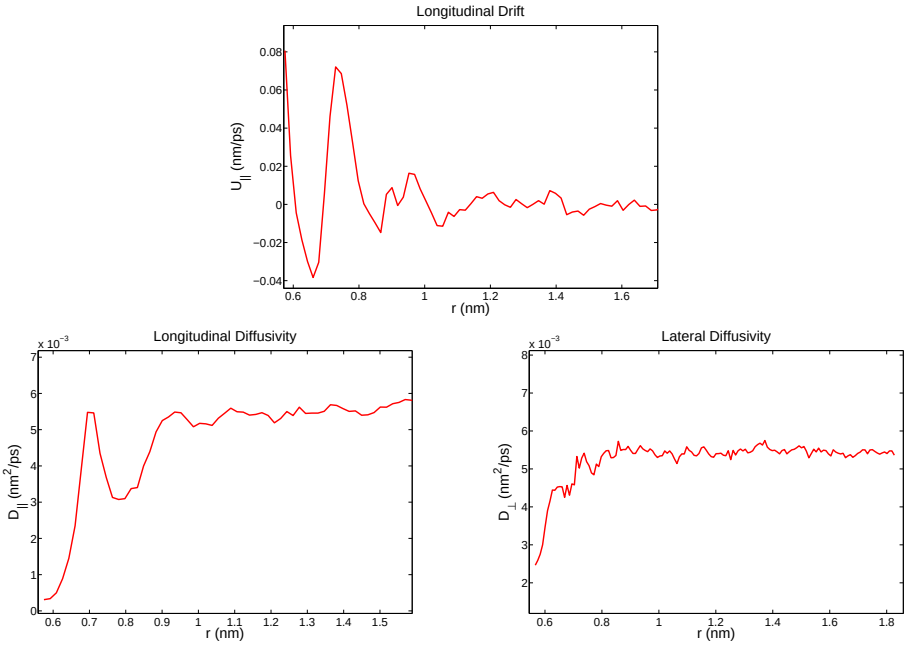


FIG. 9.5. *Parameterization of longitudinal drift (top), longitudinal diffusivity (left), and lateral diffusivity (right) from MD data with sampling time interval* $\tau = 200$ *fs.*

detailed studies of certain systems involving the interacting atoms of interest and then assumed to generalize in the codes when they are in a general, more complex molecular environment.

We did find here that the data-driven drift-diffusion model provided a means for separating features pertaining to the mean and random motion of the water molecule dynamics. One of the key limitations in the drift-diffusion modeling framework seems to be an incompatibility between the time scales over which the predictable (bias) and unpredictable (random) components of the water molecule dynamics exhibit a clean coarse-grained behavior. This forced us to choose a time scale for coarse-graining that resolved the random diffusive component well, but not the drift component. This suggests that perhaps a somewhat richer stochastic model could provide some improvement in its capacity for statistically modeling the dynamics of water molecules near a solute.

We remark that without the insight generated by the preliminary study of the toy mathematical model, we might have simply chosen a sampling time $\tau$ somewhat large compared to the momentum relaxation time scale 27 fs (as is typically done for studies of water in bulk) under the supposition that the time scale of the positional dynamics would be considerably larger. Typical choices for the sampling time scale in the literature range from $\tau \sim 200 - 1000$ fs [51, 37]. Our preliminary analysis indicated that in fact the best choice of sampling time to capture the statistics of the water dynamics would be to choose $\tau$ closer to lower end of the range 200 fs, rather than a larger value such as 1 ps $= 1000$ fs, as advocated for the biophysical diffusivity (7.1) in [37].

**Appendix A. Deterministic computations for statistics of transition properties in flashing ratchet model.**

The computation of the coefficient of variation $C_v$ and the correlation between transition time and direction $\rho_{\Theta,\Xi}$ requires consideration of the exit problem associated with the equation

$$\mathrm{d}\boldsymbol{X}(t) = -\phi'(X(t))F(t)dt + \sqrt{2\theta}\mathrm{d}W(t), \tag{A.1}$$

on a domain $[a,b]$ with $a = k+\alpha$ and $b = k+2+\alpha$, for some integer $k$, denoting the locations of the neighboring potential minima. Here $\phi(x)$ is the sawtooth potential (2.2b) and $F(t)$ is governed by a continuous-time Markov chain on the states $f_1 = 1$ and $f_2 = 0$ with transition rates $k_{12}$ and $k_{21}$. We will find it useful to denote dynamics of the Markov process $(X(t),F(t))$ corresponding to initial conditions $X(0) = x$ and $F(0) = f_i$ as $(X_{x,i}(t),F_{x,i}(t))$. Then we define the *exit time*

$$T_{x,i} = \inf\{t > 0, X_{x,i}(t) \in \{a,b\}\}$$

from the domain $[a,b]$ for a particle starting at position $x$ with the flashing potential in state $i$. The time $\Theta$ between visits to successive valley visits is statistically equivalent to $T_{x,i}$ where $x = (a+b)/2$, the location of the potential minimum which the particle has just visited. We also define the *absorption probability*

$$\pi_{+i}(x) = \mathrm{Prob}(X_{x,i}(T_{x,i}) = b)$$

corresponding to the probability for the particle to visit the potential valley to the right before the potential valley to the left; of course

$$\pi_{-i}(x) \equiv \mathrm{Prob}(X_{x,i}(T_{x,i}) = a) = 1 - \pi_{+i}(x).$$

The absorption probabilities and statistics of exit times can be computed through the solution of systems of differential equations defined by the infinitesmal generator of the governing Markov vector process $(X(t),F(t))$ [15]:

$$\mathcal{L} = -\phi'(x)\begin{bmatrix}1 & 0\\ 0 & 0\end{bmatrix}\partial_x + \theta\mathsf{I}\partial_{xx} + \mathcal{L}_f,$$

where $\mathcal{L}_f$ is the transition rate matrix

$$\mathcal{L} = \begin{pmatrix} -k_{12} & k_{12} \\ k_{21} & -k_{21}\end{pmatrix}$$

corresponding to the flashing dynamics of $F(t)$.

Writing our desired statistics as two-dimensional vectors

$$\begin{aligned}
\boldsymbol{\pi}_+(x) &= [\pi_{+1}(x),\pi_{+2}(x)]^T,\\
\bar{\boldsymbol{T}}(x) &= \mathbb{E}[T_{x,1},T_{x,2}]^T,\\
\bar{\boldsymbol{S}}(x) &= \mathbb{E}[T_{x,1}^2,T_{x,2}^2]^T,\\
\overline{\rho_{T,\Xi}}(x) &= \mathbb{E}\begin{bmatrix} T_{x,1}(I\{X_{x,1}(T_{x,1}) = b\} - I(X_{x,1}(T_{x,1}) = a\}) \\ T_{x,2}(\{I\{X_{x,2}(T_{x,2}) = b\} - I(X_{x,2}(T_{x,2}) = a)\}\end{bmatrix},
\end{aligned}$$

(where $I\{B\}$ denotes the indicator function of the event $B$), the equations to solve are as follows. For the absorption probabilities we have

$$\mathcal{L}\boldsymbol{\pi}_+(x) = \mathbf{0}, \quad \boldsymbol{\pi}_+(a) = \mathbf{0}, \boldsymbol{\pi}_+(b) = \mathbf{1}. \tag{A.2a}$$

For the mean exit time, we have

$$\mathcal{L}\bar{\boldsymbol{T}}(x) = -\mathbf{1}, \quad \bar{\boldsymbol{T}}(a) = \bar{\boldsymbol{T}}(b) = \mathbf{0}. \tag{A.2b}$$

For the second moment of the exit time, we have

$$\mathcal{L}\bar{\boldsymbol{S}}(x) = -\bar{\boldsymbol{T}}(x), \quad \bar{\boldsymbol{S}}(a) = \bar{\boldsymbol{S}}(b) = \mathbf{0}. \tag{A.2c}$$

For the basic coupling between the exit time with the escape direction (note $\mathbb{E}[T_{x,i} I\{X_{x,i}(T_{x,1}) = b\}] = \mathbb{E}[T_{x,i}(x) | X_{x,i}(T_{x,i}) = b)]\, P(X_{x,i}(T_{x,i}) = b))$, we have

$$\mathcal{L}\overline{\rho_{T,\Xi}}(x) = \boldsymbol{\pi}_-(x) - \boldsymbol{\pi}_+(x), \quad \overline{\rho_{T,\Xi}}(a) = \overline{\rho_{T,\Xi}}(b) = \mathbf{0}. \tag{A.2d}$$

Boldface numbers represent two-dimensional vectors with both entries equal to the indicated number.

These equations are solved numerically as follows. We write the operator $\mathcal{L}$ as

$$\mathsf{M}(x) \begin{bmatrix} 1 & 0 \\ 0 & 0 \end{bmatrix} \mathcal{L} = \theta \partial_x \left(\mathsf{M}(x) \partial_x\right) + \mathsf{M}(x) \mathcal{L}_f \tag{A.3}$$

with

$$\mathsf{M}(x) \equiv \begin{bmatrix} \mathrm{e}^{-\phi(x)/\theta} & 0 \\ 0 & 1 \end{bmatrix}.$$

We thereby solve equations of the form

$$\mathcal{L}\boldsymbol{g}(x) = \boldsymbol{h}(x)$$

by setting up a regular grid on the interval $[a,b]$ with interval spacing $\Delta x = (b-a)/N$, defining $x_n = a + n\Delta x$, $\boldsymbol{g}_n = \boldsymbol{g}(x_n)$, and $\boldsymbol{h}_n \approx \boldsymbol{h}(x_n)$, and then using the following *finite-volume* discretization for the equation (A.3),

$$\frac{\theta \mathsf{M}^{-1}(x_n) \mathsf{M}(x_{n+1/2})}{(\Delta x)^2} \left(\boldsymbol{g}_{n+1} - \boldsymbol{g}_n\right) - \frac{\theta \mathsf{M}^{-1}(x_n) \mathsf{M}(x_{n-1/2})}{(\Delta x)^2} \left(\boldsymbol{g}_n - \boldsymbol{g}_{n-1}\right) + \mathcal{L}_f \boldsymbol{g}_n = \boldsymbol{h}_n,$$

for $1 \le n \le N-1$, with the appropriate boundary conditions applied at $n = 0$ and $n = N$. We then use *MATLAB* for solving the resulting linear system for the vector $\boldsymbol{g} = (g_1, g_2, \ldots, g_{N-1})^T$.

With the solutions to (A.2) in hand, to compute the statistics desired in subsection 5.1 we realize that we want to choose $x = x_c \equiv (a+b)/2$ and assign $F(t)$ some appropriate initial probability distribution $p_{F,i}^{(0)} = P(F(0) = i)$. Applying the law of total expectation we then have

$$\begin{aligned}
\pi_+ &= p_{F,1}^{(0)} \pi_{+1}(x_c) + p_{F,2}^{(0)} \pi_{+2}(x_c), \\
\mathbb{E}\Theta &= p_{F,1}^{(0)} \bar{T}_1(x_c) + p_{F,2}^{(0)} \bar{T}_2(x_c), \\
\mathbb{E}\Theta^2 &= p_{F,1}^{(0)} \bar{S}_1(x_c) + p_{F,2}^{(0)} \bar{S}_2(x_c), \\
\operatorname{var}\Theta &= \mathbb{E}\Theta^2 - (\mathbb{E}\Theta)^2, \\
\mathbb{E}[\Xi\Theta] &= p_{F,1}^{(0)} \rho_{T,\Xi,1}(x_c) + p_{F,2}^{(0)} \rho_{T,\Xi,2}(x_c).
\end{aligned} \tag{A.4}$$

One might be tempted to specify the probability distribution for the initial flashing state as the stationary distribution $p^{(0)}_{F,1} = k_{21}/(k_{21}+k_{12})$, $p^{(0)}_{F,2} = k_{12}/(k_{21}+k_{12})$ [56, 8], but actually this is not appropriate here! While this probability distribution correctly describes the statistical state of the flashing ratchet potential at an arbitrary deterministic time $t$, it does not necessarily agree with the probability distribution for the state of the flashing ratchet at the *random* time at which the motor particle visits new valleys. In particular this random time is in principle correlated with the state of the flashing ratchet because of course whether the potential is on or off will affect the likelihood of the motor particle reaching the potential minimum. Consequently, we must calculate this probability distribution with some care.

To do so, we assume the motor particle behaves in an essentially ergodic manner regarding its transitions between valleys of the potential. That is, we assume the joint process $(\tilde{X}(t), F(t))$ converges to a (unique) statistically stationary process at long time, where the reduced process $\tilde{X}(t) = X(t) - \lfloor X(t) \rfloor$ simply records, at each time, the fractional part of $X(t)$, meaning its position relative to the nearest potential minimum [49]. Such a supposition is natural for an overdamped physical system driven in a statistically stationary way. Now, once we have waited long enough for the motor particle dynamics to be close to that described by this statistically stationary state, we can dissect its trajectory into a succession of statistically identical segments connecting the visit of one potential minimum to the next. Now each visit to a potential minimum is a terminating endpoint of one segment and a beginning endpoint of the next. Consequently, the probability distribution for the state of the system, including the state of the flashing ratchet, should be the same when the motor particle visits the next potential minimum as it was when the motor particle started from the previous potential minimum. That is, the probability distribution for $F(t)$ must be the same at the end of the exit problem under consideration as it is set at the initial time. We therefore set up a self-consistent calculation using absorption probability techniques [15, Sec. 5.4].

We begin by defining $\pi_{i,j}(x) = \mathrm{Prob}(F(T_{x,i}) = f_j)$ for $i,j \in \{1,2\}$ and solving the system of equations

$$\begin{aligned} -\phi'(x)\partial_x \pi_{1,i}(x) + \theta \partial_{xx} \pi_{2,i}(x) - k_{12}\pi_{1,i}(x) + k_{12}\pi_{2,i}(x) = 0, \\ \theta \partial_{xx} \pi_{2,i}(x) + k_{21}\pi_{1,i}(x) - k_{21}\pi_{2,i}(x) = 0, \end{aligned}$$

with $\pi_{i,j}(a) = \pi_{i,j}(b) = \delta_{i,j}$ using a finite volume method as described above. Equating $p^{(0)}_{F,1}$, the initialized probability for the flashing ratchet to be on when the motor particle leaves the previous valley, to the calculated probability (from the law of total expectation) for the flashing ratchet to be on at the visit to the next new valley, we obtain

$$p^{(0)}_{F,1} = \pi_{1,1} p^{(0)}_{F,1} + \pi_{1,2} p^{(0)}_{F,2} = \pi_{1,1} p^{(0)}_{F,1} + \pi_{1,2}(1 - p^{(0)}_{F,1}),$$

and therefore

$$p^{(0)}_{F,1} = \pi_{1,2}/(1 - \pi_{1,1} + \pi_{1,2}).$$

In figure A.1, we plot this probability for two choices of $\theta$ and various transition rates $k_{21} = k_{12} = \nu$; it is clearly different from the value of 0.5 corresponding to the stationary distribution of $F(t)$ at a deterministic time $t$. For these calculations, we are taking the flashing states as $f_1 = 1$ and $f_2 = -1$ to provide more direct comparison with the results of [8]. We also show that our deterministic calculation for the mean exit

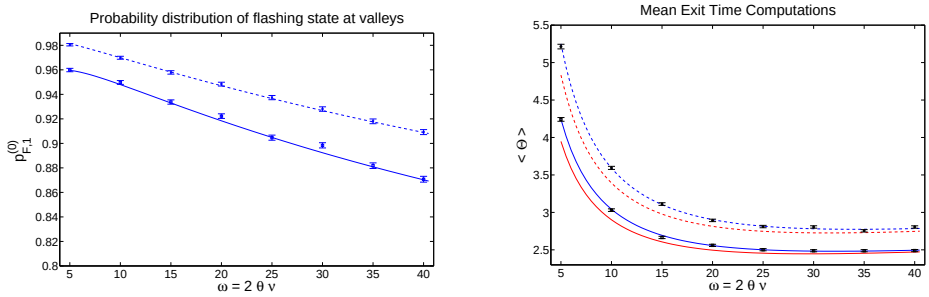


FIG. A.1. *(left) Computation of* $p^{(0)}_{F,1}$ *through deterministic approach and Monte Carlo simulations for* $\theta = 1/7$ *(solid line) and* $\theta = 1/9$ *(dashed line). (right) Computation of mean exit time* $\langle \Theta \rangle$ *through deterministic approach with* $p^{(0)}_{F,1}$ *computed self-consistently (blue) and with* $p^{(0)}_{F,1}$ *computed using stationary distribution* $p^{(0)}_{F,1} = 1/2$ *as in [8] (red). Again, the solid lines correspond to* $\theta = 1/7$ *and the dashed lines to* $\theta = 1/9$*. The results of Monte Carlo simulations are plotted with error bars corresponding to one sample standard deviation. In these figures,* $k_{21} = k_{12} = \nu$ *and the states of the flashing ratchet are* $f_1 = 1$ *and* $f_2 = -1$*.*

TABLE A.1. *Comparison for exit time problems between theoretical values and Monte Carlo sampling ("MC").* $\theta = 10^{-1.1}$*. The reported uncertainties correspond to one standard deviation.*

| $(k_{12}, k_{21})$ | $\langle \Theta \rangle$ | $\langle \Theta \rangle (MC)$ | $\mathrm{var}\,\Theta$ | $\mathrm{var}\,\Theta (MC)$ |
|---|---|---|---|---|
| $(10^{-1.7}, 10^{0})$ | 183 | $183 \pm 1$ | $3.8 \times 10^4$ | $(3.8 \pm 0.8) \times 10^4$ |
| $(10^{-1.2}, 10^{0.4})$ | 114.3 | $114.6 \pm 0.8$ | $8.4 \times 10^3$ | $(1.3 \pm 0.3) \times 10^4$ |
| $(10^{-0.7}, 10^{0.8})$ | 80.0 | $79.3 \pm 0.6$ | $6.2 \times 10^3$ | $(6.1 \pm 0.1) \times 10^3$ |

| $(k_{12}, k_{21})$ | $\pi_+ - \pi_-$ | $\pi_+ - \pi_- (MC)$ |
|---|---|---|
| $(10^{-1.7}, 10^{0})$ | 0.623 | $0.626 \pm 0.006$ |
| $(10^{-1.2}, 10^{0.4})$ | 0.841 | $0.851 \pm 0.004$ |
| $(10^{-0.7}, 10^{0.8})$ | 0.952 | $0.947 \pm 0.002$ |

time produces excellent agreement with Monte Carlo simulations, though interestingly simply using the stationary distribution value for $p^{(0)}_{F,1}$ does not seem to create too much of an error.

As another validation of our computation of statistics, we display in Table A.1 some comparison between our theoretical computations and Monte Carlo simulations. Sample points are presented from each of the regions $C_v > 1$, $C_v \approx 1$, and $C_v < 1$. Again, the Monte Carlo simulations are much more expensive and less accurate than our deterministic computations.

**Acknowledgement.** The authors would like to thank Grigorios Pavliotis for his creative input into theoretical questions regarding the molecular motor modeling work and computational framework and Eric Vanden-Eijnden for stimulating discussions. We particularly acknowledge Shekhar Garde for his intellectual stimulation regarding the stochastic modeling of water molecules near protein surfaces and his research group's contribution of molecular dynamics simulations and helpful collaboration regarding their analysis.

## REFERENCES

[1] R.D. Astumian and P. Hänggi, *Brownian motors*, Physics Today, 33–39, 2002.
[2] M.C. Bellissent-Funel, *Hydration Processes in Biology. Theoretical and Experimental Approaches*, NATO Science Series, Amsterdam, NATO Advanced Study Institute, IOS Press, 1999.
[3] A.N. Borodin and P. Salminen, *Handbook of Brownian Motion—Facts and Formulae*, Probability and its Applications, Birkhäuser Verlag, Basel, second edition, section II.3, 672, 2002.
[4] V.P. Denisov, K. Venu, J. Peters, H.D. Hörlein and B. Halle, *Orientational disorder and entropy of water in protein cavities*, J. Phys. Chem. B, 101, 9380–9389, 1997.
[5] J.M. Deutch and I. Oppenheim, *The concept of Brownian motion in modern statistical mechanics*, Brownian Motion, Faraday Discuss. Chem. Soc., London, The Faraday Division of the Royal Society of Chemistry, The Royal Society of Chemistry, 83, 1–20, 1987.
[6] R.E.L. DeVille and E. Vanden-Eijnden, *Regular gaits and optimal velocities for motor proteins*, Biophysical Journal, 95, 2681–2691, 2008.
[7] R.E.L. DeVille and E. Vanden-Eijnden, *Regularity and synchrony in motor proteins*, Bull. Math. Biol., 70, 484–516, 2008.
[8] A.A. Dubkov and B. Spagnolo, *Acceleration of diffusion in randomly switching potential with supersymmetry*, Phys. Rev. E, 72, 041104, 2005.
[9] T.C. Elston, *A macroscopic description of biomolecular transport*, J. Math. Biology, 41, 189–206, 2000.
[10] T.C. Elston and C.S. Peskin, *The role of protein flexibility in molecular motor function: coupled diffusion in a tilted periodic potential*, SIAM J. Appl. Math., 60, 842–867, (electronic) 2000.
[11] T.C. Elston, D. You and C.S. Peskin, *Protein flexibility and the correlation ratchet*, SIAM J. Appl. Math., 61, 776–791, (electronic) 2000.
[12] C.P. Fall, E.S. Marland, J.M. Wagner and J.J. Tyson, *Computational Cell Biology*, Interdisciplinary Applied Mathematics, Springer-Verlag, New York, 20, 2002.
[13] M.E. Fisher and A.B. Kolomeisky, *Simple mechanochemistry describes the dynamics of kinesin molecules*, Proceedings of the National Academy of Sciences, 98, 7748–7753, 2001.
[14] D. Frenkel and B. Smit, *Understanding Molecular Simulation – From Algorithms to Applications*, Academic Press, New York, 1996.
[15] C.W. Gardiner, *Handbook of Stochastic Methods*, second edition, Springer Series in Synergetics, Springer-Verlag, Berlin, 13, 1985.
[16] M. Gerstein and M. Levitt, *Simulating water and the molecules of life*, Scientific American, 100–105, 1998.
[17] B. Halle, *Water in biological systems: the NMR picture*, Bellissent-Funel [2], 233–249.
[18] P. Hänggi and F. Marchesoni, *Artificial Brownian motors: controlling transport on the nanoscale*, Rev. Mod. Phys., 81, 387–442, 2009.
[19] F. Jülicher, A. Ajdari and J. Prost, *Modeling molecular motors*, Rev. Mod. Phys., 69, 1269–1281, 1997.
[20] A. Kalra, G. Hummer and S. Garde, *Methane partitioning and transport in hydrated carbon nanotubes*, J. Phys. Chem. B, 108, 544–549, 2004.
[21] S. Karlin and H.M. Taylor, *A First Course in Stochastic Processes*, Academic Press, Boston, second edition, 1975.
[22] M. Karplus and J.A. McCammon, *The dynamics of proteins*, Scientific American, 254, 42–51, 1986.
[23] D. Kinderlehrer and M. Kowalczyk, *Diffusion-mediated transport and the flashing ratchet*, Arch. Ration. Mech. Anal., 161, 149–179, 2002.
[24] P.E. Kloeden and E. Platen, *Numerical Solution of Stochastic Differential Equations*, Applications of Mathematics: Stochastic Modelling and Applied Probability, Springer-Verlag, Berlin, 23, 1992.

[25] A.B. Kolomeisky and M.E. Fisher, *A simple kinetic model describes the processivity of Myosin-V*, Biophys. J., 84, 1642–1650, 2003.
[26] A.B. Kolomeisky and M.E. Fisher, *Molecular motors: a theorist's perspective*, Annual Review of Physical Chemistry, 58, 675–695, 2007.
[27] M. Kostur, *Numerical approach to Fokker-Planck equations for Brownian motors*, International J. Modern Physics C, 13, 1157–1176, 2002.
[28] J.C. Latorre, P.R. Kramer and G.A. Pavliotis, *Effective transport properties for flashing ratchets using homogenization theory*, PAMM, 7, 1080501-1080502, 2008. Special Issue: Sixth International Congress on Industrial Applied Mathematics (ICIAM07) and GAMM Annual Meeting, Zürich 2007.
[29] C.Y. Lee, J.A. McCammon and P.J. Rossky, *The structure of liquid water at an extended hydrophobic surface*, J. Chem. Phys., 80, 4448–4455, 1984.
[30] R.E. Lee DeVille and E. Vanden-Eijnden, *Self-induced stochastic resonance for Brownian ratchets under load*, Commun. Math. Sci., 5, 431–446, 2007.
[31] J. Lehmann, P. Reimann and P. Hänggi, *Activated escape over oscillating barriers: the case of many dimensions*, Phys. Stat. Sol., 237, 53–71, 2003.
[32] B. Lindner, M. Kostur and L. Schimansky-Geier, *Optimal diffusive transport in a tilted periodic potential*, Fluctuation and Noise Letters, 1, R25–R39, 2001.
[33] V. Lounnas, *Molecular dynamics simulation of proteins in aqueous environment*, in Bellissent-Funel [2], 261–290.
[34] V. Lounnas, B.M. Pettitt and J. George N. Phillips, *A global model of the protein-solvent interface*, Biophys. J., 66, 601–614, 1994.
[35] C. Maes and M.H. van Wieren, *A Markov model for kinesin*, J. Stat. Phys., 112, 329–355, 2003.
[36] V.A. Makarov, *Residence times of water molecules in the hydration sites of myoglobin*, Biophys. J., 79, 2966–2974, 2000.
[37] V.A. Makarov, M. Feig, B.K. Andrews and B.M. Pettitt, *Diffusion of solvent around biomolecular solutes: a molecular dynamics simulation study*, Biophys. J., 75, 150–158, 1998.
[38] C. Mattos, *Protein-water interactions in a dynamic world*, TRENDS in Biochemical Sciences, 27, 203–208, 2002.
[39] D.A. McQuarrie, *Statistical Mechanics*, University Science Books, Herndon, VA, second edition, 2000.
[40] A. Mogilner, T.C. Elston, H. Wang and G. Oster, *Molecular motors: theory*, in Fall et al. [12], chapter 12, 68.
[41] J. Munárriz, J.J. Mazo and F. Falo, *Model for hand-over-hand motion of molecular motors*, Phys. Rev. E, 77, 031915, 2008.
[42] A. Papavasiliou, G.A. Pavliotis and A.M. Stuart, *Maximum likelihood drift estimation for multiscale diffusions*, Stoch. Proc. and Appl., in press.
[43] J.M.R. Parrondo and B.J. de Cisneros, *Energetics of Brownian motors: a review*, Appl. Phys. A, 75, 179–191, 2002.
[44] R.K. Pathria, *Statistical Mechanics*, Pergamon Press, Oxford, section 13.4, 1972.
[45] G.A. Pavliotis, *A multiscale approach to Brownian motors*, Phys. Lett. A, 344, 331–345, 2005.
[46] G.A. Pavliotis, Y. Pokern and A.M. Stuart, *Parameter estimation for multiscale diffusions: An overview*, Proceedings of SemStat2007, LaManga, Sept. 19, to appear, 2009.
[47] G.A. Pavliotis and A.M. Stuart, *Parameter estimation for multiscale diffusions*, J. Stat. Phys., 127, 741–781, 2007.
[48] H. Qian, *The mathematical theory of molecular motor movement and chemomechanical energy transduction*, J. Math. Chem., 27, 219–234, 2000.
[49] P. Reimann, *Brownian motors: noisy transport far from equilibrium*, Phys. Rep., 361, 57, 2002.
[50] P. Reimann and P. Hänggi, *Introduction to the physics of Brownian motors*, Appl. Phys. A, 75, 169–178, 2002.
[51] C. Rocchi, A.R. Bizarri and S. Cannistraro, *Water dynamical anomalies evidenced by molecular-dynamics simulations at the solvent-protein interface*, Phys. Rev. E, 57, 3315–3325,1998.
[52] C. Rocchi, A.R. Bizzarri and S. Cannistraro, *Water residence times around copper plastocyanin: a molecular dynamics simulation approach*, J. Chem. Phys., 214, 261–276, 1997.
[53] M.J. Schilstra and S.R. Martin, *An elastically tethered viscous load imposes a regular gait on the motion of myosin-V. Simulation of the effect of transient force relaxation on a stochastic process*, Journal of The Royal Society Interface, 3, 153–165, 2006.
[54] T. Schlick, *Molecular Modeling and Simulation: An Interdisciplinary Guide*, Interdisciplinary Applied Mathematics, Springer-Verlag, Berlin, 21, 2002.

[55] T. Schlick, R.D. Skeel, A.T. Brunger, L.V. Kalé, J.A. Board, Jr., J. Hermans and K. Schulten, *Algorithmic challenges in computational molecular biophysics*, J. Comput. Phys., 151, 9–48, 1999.

[56] B. Spagnolo, A.A. Dubkov and N.V. Agudov, *Escape times in fluctuating metastable potential and acceleration of diffusion in periodic fluctuating potentials*, Physica A, 340, 265–273, 2004.

[57] H. Wang, *A new derivation of the randomness parameter*, J. Math. Phys., 48, 103301, 18, 2007.

[58] H. Wang and T.C. Elston, *Mathematical and computational methods for studying energy transduction in protein motors*, J. Stat. Phys., 128, 35–76, 2007.

[59] H. Wang, C.S. Peskin and T.C. Elston, *A robust numerical algorithm for studying biomolecular transport processes*, J. Theoret. Biol., 221, 491–511, 2003.